

Single Event Effects Testing of the ISL70417SEH, Quad 40V Rad Hard Precision Operation Amplifiers

Introduction

The intense heavy ion environment encountered in space applications can cause a variety of transient and destructive effects in analog circuits, including single-event latch-up (SEL), single-event transients (SET) and single-event burnout (SEB). These effects can lead to system-level failures including disruption and permanent damage. For predictable and reliable system operation, these components have to be formally designed and fabricated for SEE hardness, followed by detailed SEE testing to validate the design. This report discusses the results of SEE testing of Intersil's ISL70417SEH.

Related Documents

- ISL70417SEH Data Sheet, [FN7962](#)
- ISL70417SEH Radiation Report, [AN1792](#)

Product Description

The ISL70417SEH contains four very high precision amplifiers featuring the perfect combination of low noise vs power consumption. These devices are fabricated in a 40V advanced bonded wafer SOI process using deep trench isolation, resulting in a fully isolated structure. This choice of process technology also results in latch-up free performance, whether electrically or single event (SEL) induced.

A super-beta NPN input stage with input bias current cancellation provides low input bias current, low input offset voltage, low input noise voltage, and low 1/f noise corner frequency. These amplifiers also feature high open loop gain for excellent CMRR and THD+N performance. A complementary bipolar output stage enables high capacitive load drive without external compensation.

This amplifier is designed to operate over a wide supply range of 4.5V to 40V. Applications for these amplifiers include precision active filters, low noise front ends, loop filters, data acquisition and charge amplifiers.

The combination of high precision, low noise, low power and radiation tolerance provides the user with outstanding value and flexibility relative to similar competitive parts.

The part is packaged in a 14 lead hermetic ceramic flat pack and operates over the extended temperature range of -55 °C to +125 °C. A summary of key full temperature range specifications follows:

- Input Offset Voltage 110µV, max.
- Offset Voltage Drift 1µV/°C, max.
- Input Offset Current 3nA, max.
- Input Bias Current 5nA, max.
- Supply Current/Amplifier 0.68mA, max.
- Gain Bandwidth Product 1.5MHz, typ.

Key SEE Test Results

- SOI process for latch-up immunity
- No single event burnout up to 40V supply range
- Ultra low cross section for significant SETs:
 - $V_S = \pm 5V$: $1.75 \times 10^{-5} \text{ cm}^2$
 - $V_S = \pm 15V$: $1.15 \times 10^{-5} \text{ cm}^2$
- Offers a lower cross section at similar gain and LET than the RH1014

SEE Test Objective

The objectives of SEE testing of the ISL70417SEH were to evaluate its susceptibility to destructive events induced by single event effects, such as single event burnout and to determine its SET behavior.

SEE Test Facility

Testing was performed at the Texas A&M University (TAMU) Cyclotron Institute heavy ion facility. This facility is coupled to a K500 super-conducting cyclotron, which is capable of generating a wide range of test particles with the various energy, flux and fluence levels needed for advanced radiation testing.

SEE Test Procedure

The part was tested for single event burnout, using Xe ions at 45 °C incidence ($LET = 73.9 \text{ MeV} \cdot \text{cm}^2/\text{mg}$) with a case temperature of 125 °C, and single event transient characterized using Ne, Ar, and Kr ions with a case temperature of 25 °C.

The device under test (DUT) was mounted in the beam line and irradiated with heavy ions of the appropriate species. The parts were assembled in 14 lead dual in-line packages with the metal lid removed for beam exposure. The beam was directed onto the exposed die and the beam flux, beam fluence and errors in the device outputs were measured.

The tests were controlled remotely from the control room. All input power was supplied from portable power supplies connected via cable to the DUT. The supply currents were monitored along with the device outputs. All currents were measured with digital ammeters, while all the output waveforms were monitored on a digital oscilloscope for ease of identifying the different types of SEE, displayed by the part. Events were captured by triggering on changes in the output.

SEE Test Set-Up Diagrams

A schematic of the evaluation board used during testing is shown in Figure 1.

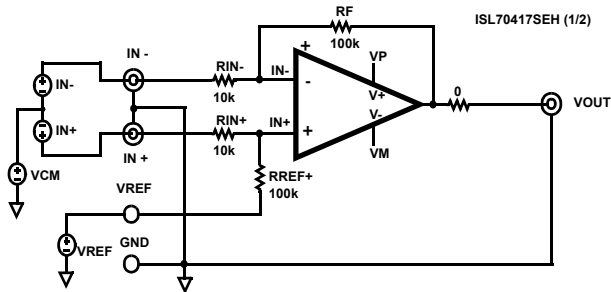


FIGURE 1. ISL70417SEH SEE TEST SCHEMATIC

Each operational amplifier was set up in a non-inverting operation with $G = 10V/V$. The IN- inputs were grounded and the input signal was applied to the IN+ pin. The reference input was also grounded. The complete board schematic and silk screen of the top of the board are included in Appendix A.

Cross Section Calculation

Cross sections (CS) are calculated as shown by Equation 1:

$$CS (LET) = N/F \quad (EQ. 1)$$

where:

- CS is the SET cross section (cm^2), expressed as a function of the heavy ion LET
- LET is the linear energy transfer in $MeV \cdot cm^2/mg$, corrected according to the incident angle, if any
- N is the total number of SET events
- F is fluence in particles/ cm^2

A value of $1/F$ is the assumed cross section when no event is observed.

Single Event Burnout Results

The first testing sequence looked at destructive effects due to burnout. A burnout condition is indicated by a permanent change in the device supply current after application of the beam. If the increased current can be reset by cycling power, it is termed a latch-up. No burnout was observed using Xe ions at $45^\circ C$. Testing was performed on four parts at $T_C = +125^\circ C$ and up to the maximum voltage, $V_S = \pm 20V$. The first two parts (part ID 1 & 2) commenced testing with $V_S = \pm 18V$ and on subsequent tests V_S voltage was increased until $V_S = \pm 20V$ was achieved. The last two parts were tested with a V_S of $\pm 18.4V$ and $\pm 20V$. All test runs were run to a fluence of $2 \times 10^6/cm^2$. A power supply applied a DC voltage of 200mV to the non-inverting inputs of the amplifiers during the test. Functionality of all outputs was verified after exposure. I_{DD} and I_{EE} were recorded pre and post exposure and summed up. A 5% change in total supply current indicates permanent damage to the op amp. Test results are shown in Table 1 for the 40V total supply voltage.

Single Event Transient Results

Test Setup

Biasing used for SET test runs was $V_S = \pm 5V$ and $\pm 15V$. Similar to SEL/B testing, a DC voltage of 200mV was applied to the non-inverting inputs of the amplifiers. Signals from the switch board in the control room were connected to four LECROY oscilloscopes. Summary of the scope settings are as follows:

TRIGGER CONNECTIONS:

- Scope 1 is set to trigger on Channel 1
- Scope 2 is set to trigger on Channel 2
- Scope 3 is set to trigger on Channel 3
- Scope 4 is set to trigger on Channel 4

CHANNEL CONNECTION ON ALL SCOPES FOR $V_S = \pm 5V$:

- CH1 = OUTA 1V/div, CH2 = OUTB 1V/div
- CH3 = OUTC 1V/div, CH4 = OUTD 1V/div

CHANNEL CONNECTION ON ALL SCOPES FOR $V_S = \pm 15V$:

- CH1 = OUTA 2V/div, CH2 = OUTB 2V/div
- CH3 = OUTC 2V/div, CH4 = OUTD 2V/div

SET events are recorded when movement on output during beam exposure exceeds the set window trigger of $\pm 200mV$ for $V_S = \pm 5V$ and $\pm 400mV$ for $V_S = \pm 15V$. The trigger window was modified as a result of the changing the scale for the higher supply voltage in order to capture the complete transients. The switch board at the end of the 20-ft cabling was found to require terminations of 10nF to keep the noise on the waveforms to a minimum.

Cross Section Results

Compared to other Intersil radiation tolerant circuits, the ISL70417SEH was not designed for single event transient (SET) mitigation. The best approach to characterize the SET response is to represent the data on a LET threshold plot. Figure 2 shows the cross section of the IC versus the LET level, at $V_S = \pm 5V$ and $\pm 15V$. It can be seen that for an $LET < 5.4 MeV \cdot cm^2/mg$, the cross section is lower with a higher supply voltage. As the LET increases with the use of Ar ions, the higher supply voltage exhibits a larger cross section. However, with Kr ions the cross section areas merge. Data from Figure 2 is represented in Table 2. Figures 3 through 10 show the cross section of each channel independently at $V_S = \pm 5V$ and $\pm 15V$ with confidence interval bars for a 90% confidence level. The graphs also show that there is no channel-to-channel sensitivity. Complete data for these figures is available in Appendix A.

Single Event Effects Testing of the ISL70417SEH,
Quad 40V Rad Hard Precision Operation Amplifiers

TABLE 1. ISL70417SEH DETAILS OF SEB/L TESTS FOR $V_S = \pm 20V$ and $LET = 73.9MeV \cdot cm^2/mg$

TEMP (°C)	LET (MeV . cm ² /mg)	SUPPLY CURRENT PRE-EXPOSURE (mA)	SUPPLY CURRENT POST-EXPOSURE (mA)	DESTRUCTIVE EVENTS	CUMULATIVE FLUENCE (PARTICLES/cm ²)	CUMULATIVE CROSS SECTION (cm ²)	DEVICE ID	SEB
+125	73.9	4.201	4.201	0	2.0×10^6	5.0×10^{-7}	1	PASS
+125	73.9	4.349	4.347	0	2.0×10^6	5.0×10^{-7}	2	PASS
+125	73.9	4.217	4.217	0	2.0×10^6	5.0×10^{-7}	3	PASS
+125	73.9	4.215	4.216	0	2.0×10^6	5.0×10^{-7}	4	PASS
TOTAL EVENTS				0				
OVERALL FLUENCE					8.0×10^6			
OVERALL CS						1.25×10^{-7}		
TOTAL UNITS							4	

TABLE 2. DETAILS OF THE LET THRESHOLD PLOT OF THE ISL70417SEH

SUPPLY VOLTAGE (V)	ION	ANGLE	EFFECTIVE LET (MeV . cm ² /mg)	FLUENCE PER RUN (PARTICLES/cm ²)	NUMBER OF RUNS	TOTAL SET	EVENT CS (cm ²)
±5	Ne	0	2.7	2.0×10^6	4	392	4.90×10^{-5}
±5	Ar	0	8.5	2.0×10^6	4	1789	2.24×10^{-4}
±5	Ar	45	12	2.0×10^6	4	2072	2.59×10^{-4}
±5	Kr	0	28	2.0×10^6	4	4852	1.21×10^{-3}
±5	Kr	50	44	1.0×10^6	4	4683	2.34×10^{-3}
±15	Ne	0	2.7	2.0×10^6	4	239	2.99×10^{-5}
±15	Ar	0	8.5	2.0×10^6	4	2957	3.70×10^{-4}
±15	Ar	45	12	2.0×10^6	4	4118	5.15×10^{-4}
±15	Kr	0	28	2.0×10^6	4	8643	1.08×10^{-3}
±15	Kr	50	44	1.0×10^6	4	6476	1.62×10^{-3}

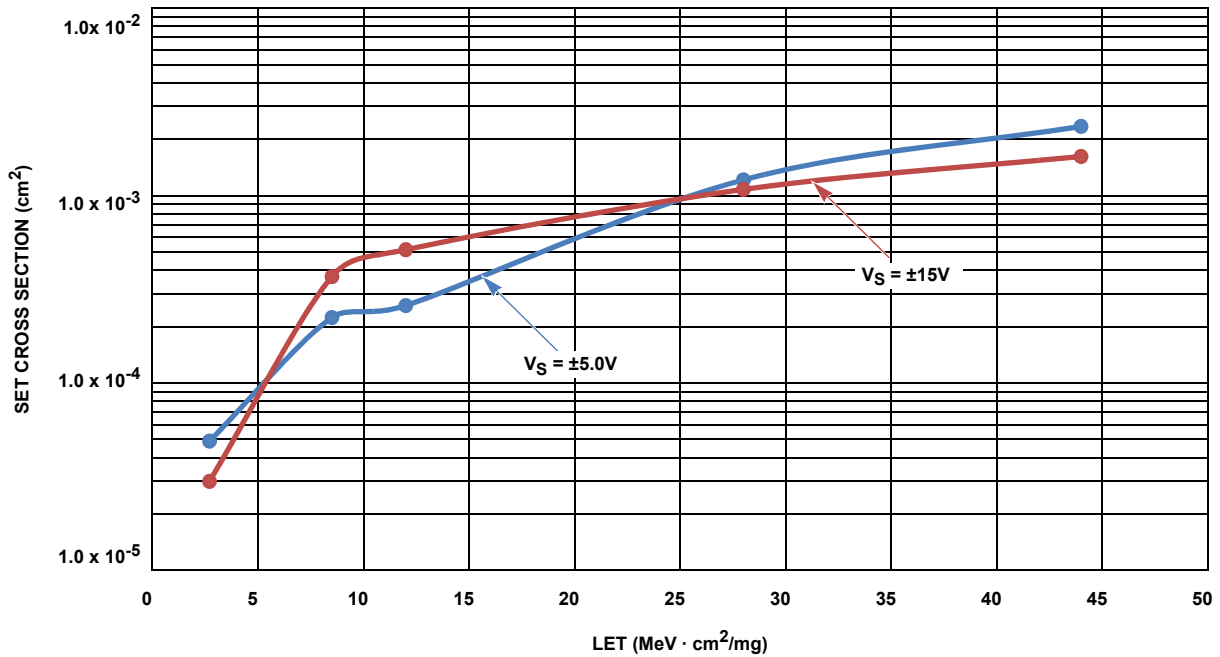


FIGURE 2. SET CROSS SECTION vs LINEAR ENERGY TRANSFER vs SUPPLY VOLTAGE

SEE Report Performance Curves

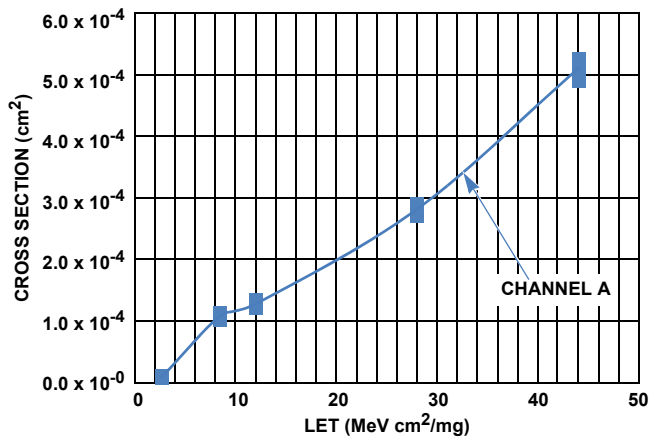


FIGURE 3. CHANNEL A SET CROSS SECTION vs LET FOR $V_S = \pm 5V$ WITH 90% CONFIDENCE LEVEL INTERVAL BARS

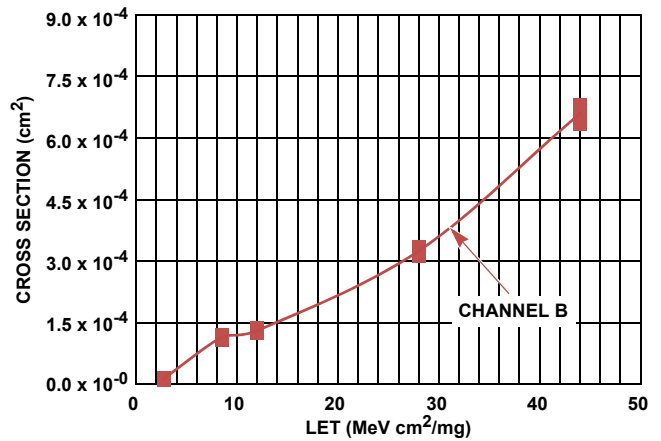


FIGURE 4. CHANNEL B SET CROSS SECTION vs LET FOR $V_S = \pm 5V$ WITH 90% CONFIDENCE LEVEL INTERVAL BARS

SEE Report Performance Curves (Continued)

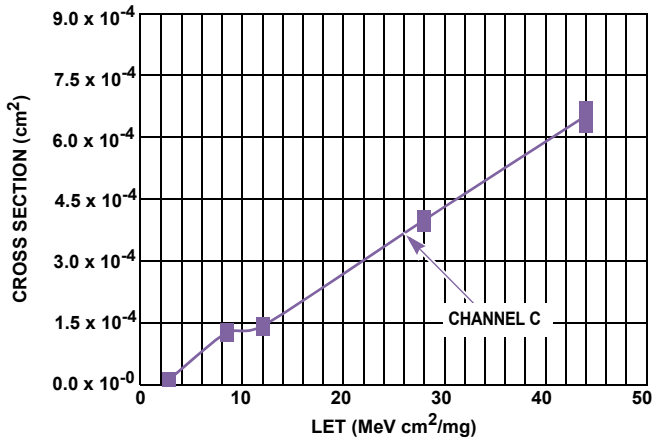


FIGURE 5. CHANNEL C SET CROSS SECTION vs LET FOR $V_S = \pm 5V$ WITH 90% CONFIDENCE LEVEL INTERVAL BARS

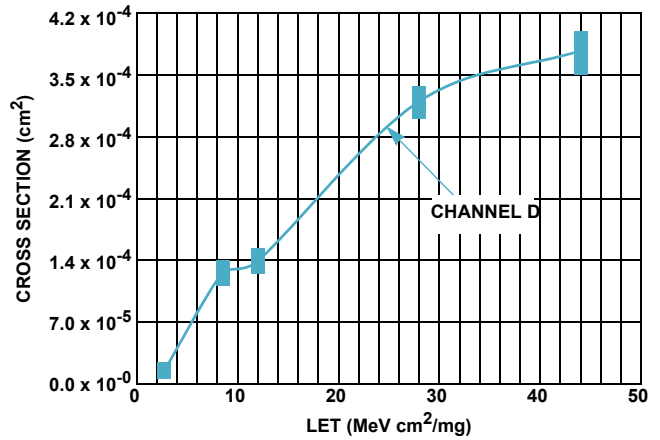


FIGURE 6. CHANNEL D SET CROSS SECTION vs LET FOR $V_S = \pm 5V$ WITH 90% CONFIDENCE LEVEL INTERVAL BARS

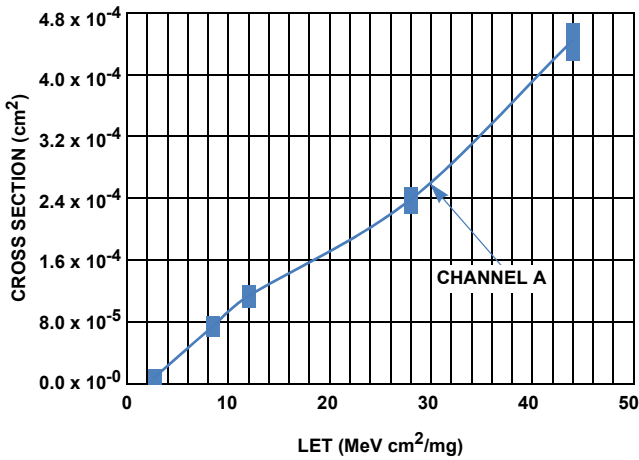


FIGURE 7. CHANNEL A SET CROSS SECTION vs LET FOR $V_S = \pm 15V$ WITH 90% CONFIDENCE LEVEL INTERVAL BARS

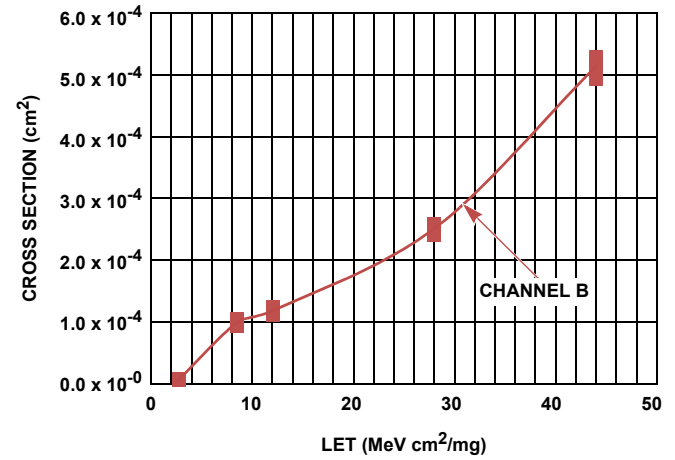


FIGURE 8. CHANNEL B SET CROSS SECTION vs LET FOR $V_S = \pm 15V$ WITH 90% CONFIDENCE LEVEL INTERVAL BARS

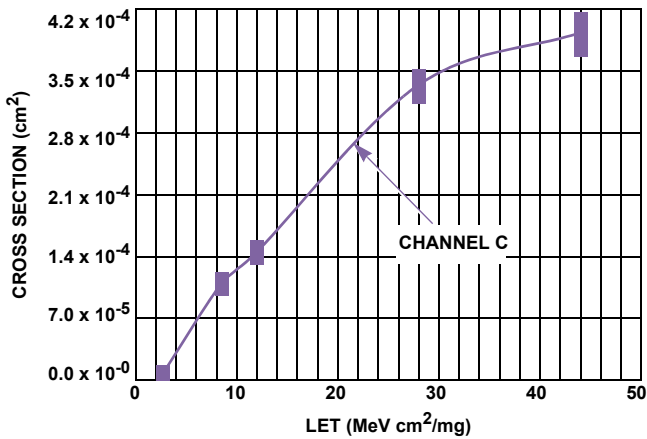


FIGURE 9. CHANNEL C SET CROSS SECTION vs LET FOR $V_S = \pm 15V$ WITH 90% CONFIDENCE LEVEL INTERVAL BARS

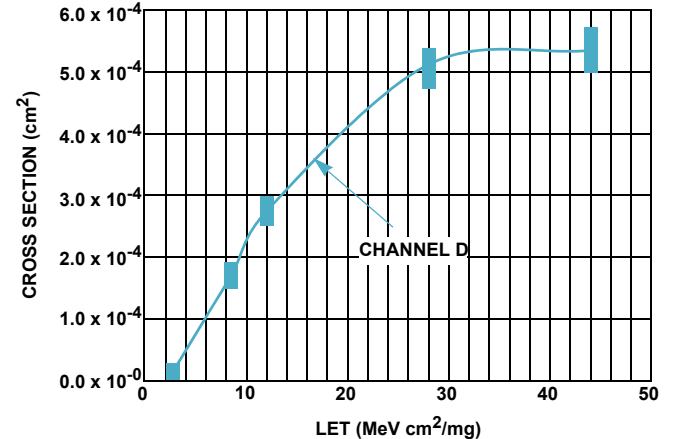


FIGURE 10. CHANNEL D SET CROSS SECTION vs LET FOR $V_S = \pm 15V$ WITH 90% CONFIDENCE LEVEL INTERVAL BARS

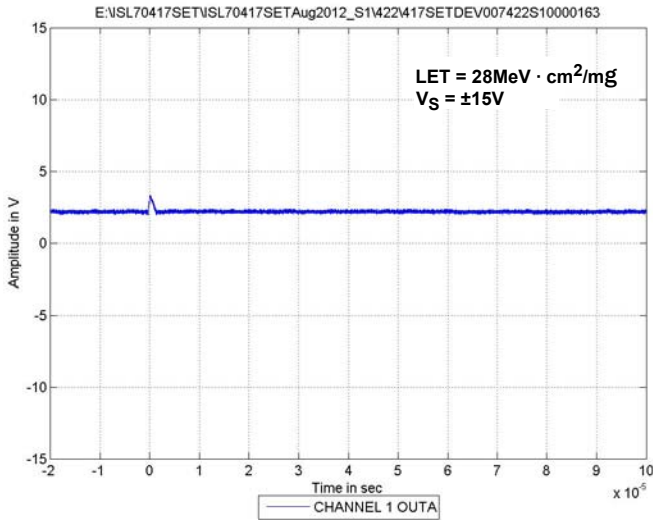


FIGURE 11. EXAMPLE POSITIVE TRANSIENT

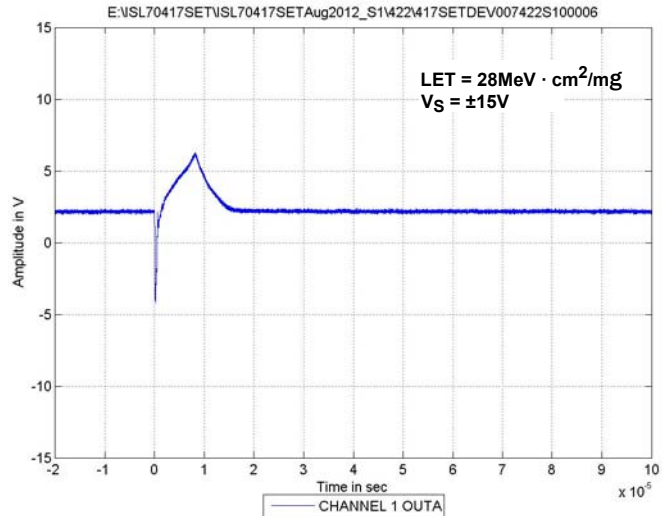


FIGURE 13. EXAMPLE SHORT POSITIVE AND NEGATIVE TRANSIENT

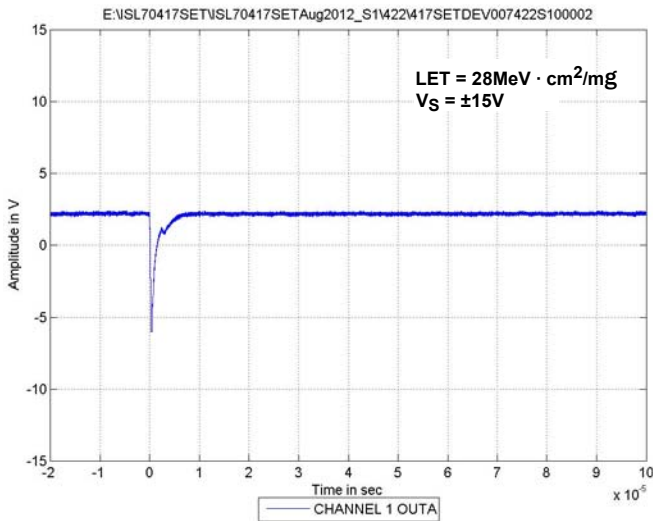


FIGURE 12. EXAMPLE NEGATIVE TRANSIENT

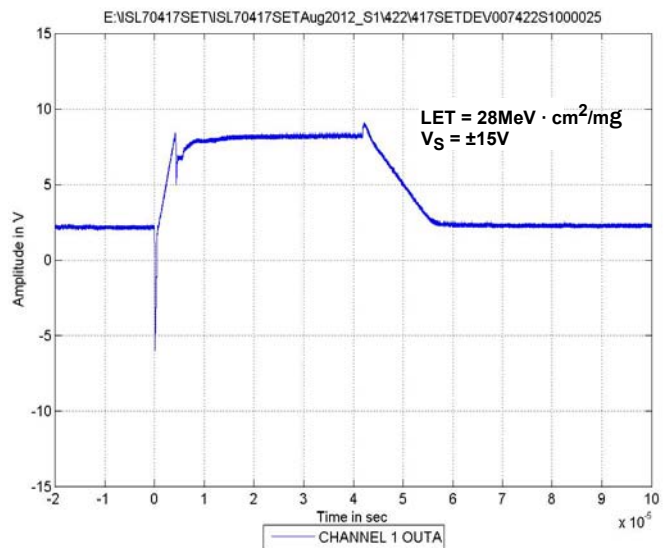


FIGURE 14. EXAMPLE LONG POSITIVE AND NEGATIVE TRANSIENT

Single Event Transient Response

The captured single event transients had a variety of amplitudes and widths. There are both positive and negative transients on most of the captures, while the rest of the transients were either positive or negative. Figures 11 through 14 give an example of each type of transient observed during SET testing.

The magnitude of the SET is proportional to the LET value; the higher the LET value the larger the peak voltage deviation, while the widths of single event transients are independent of the LET value. The response could be explained by the fact that higher LETs inject more charge into the silicon (probably the biasing network) therefore directly influencing the magnitude of deviation, but the time to recover is strictly due to the speed of the op amp (slew rate) which a varying LET level has no effect on.

Note in the tests with $V_S = \pm 5V$, the higher LETs do produce a larger magnitude in deviation however since the ISL70417SEH is not a rail to rail IC, the output saturates to the V_{OH} level for LETs greater than 8.5.

Figure 15 shows a histogram plot of the magnitude of the SET versus LET for channels biased at $\pm 5V$. For LET 2.7 the peak magnitude is 1.6V, for LET 8.5 there peak is 2V and it only occurred once. As the LET increases the peak is still 2V however the occurrences are more common.

Figure 16 shows a histogram plot of the peak positive deviations for channel 1 and $V_S = \pm 15V$. Since this bias condition allows for a V_{OH} level of 13.5V, relationship of LET vs SET magnitude is clearly seen. At an LET = 2.7 the peak voltage deviation is 1.5V, for 8.5 LET the peak voltage deviation increases to 5.5V, and as the LET increases so the magnitude of the deviation as an LET of 44 has peak deviations that are 8.5V in magnitude.

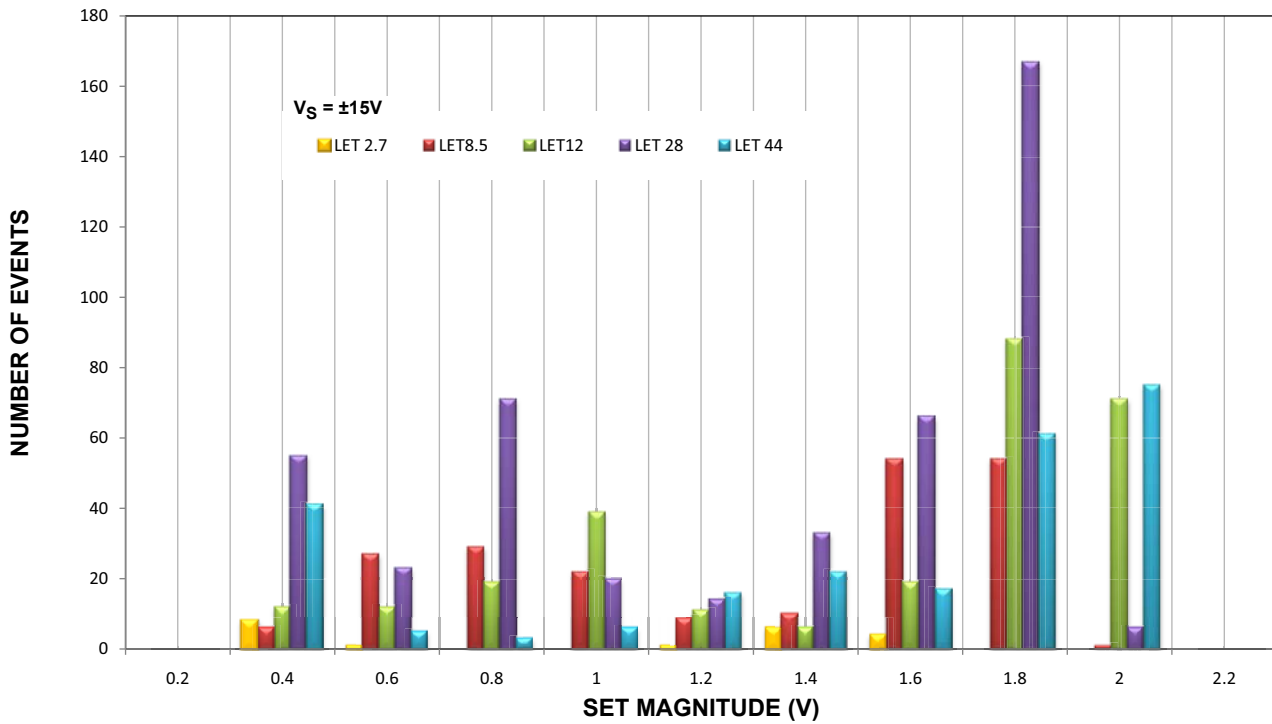


FIGURE 15. SET MAGNITUDE vs LINEAR ENERGY TRANSFER FOR $V_S = \pm 15V$

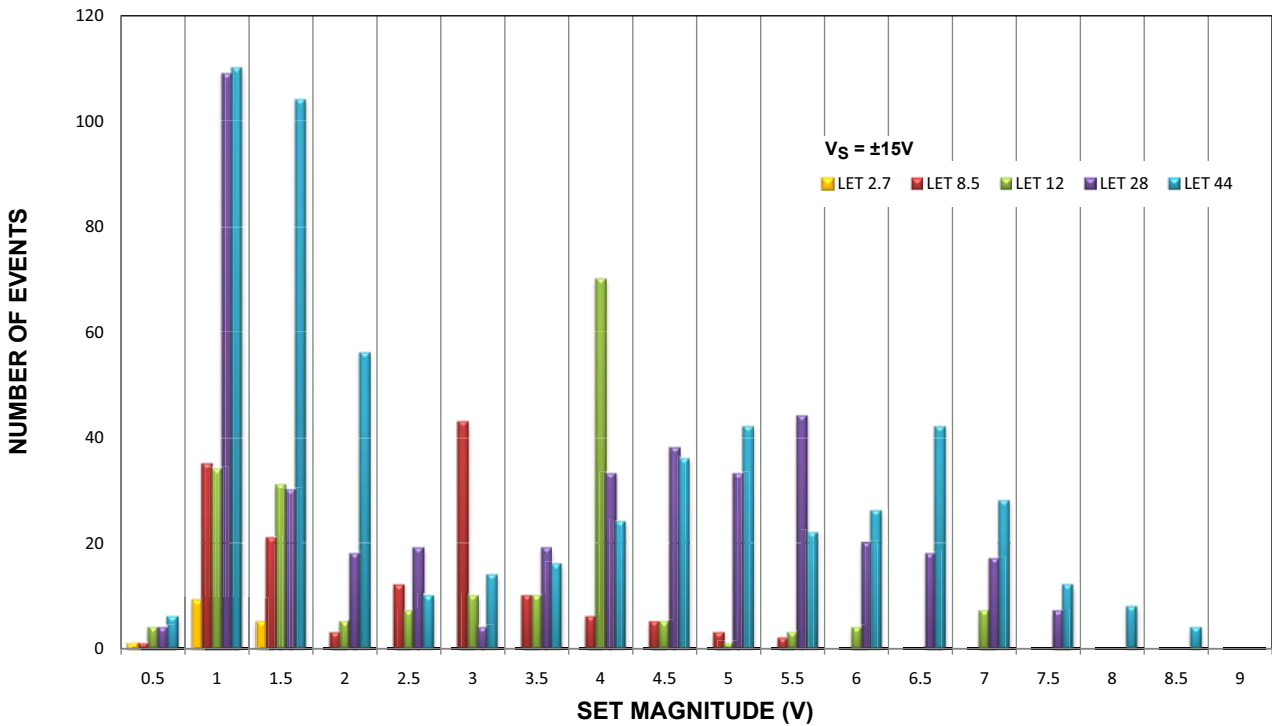


FIGURE 16. SET MAGNITUDE vs LINEAR ENERGY TRANSFER vs FOR $V_S = \pm 15V$

There was a correlation to the duration of the SET with respect to the supply voltage; the lower supply voltage exhibited a shorter SET duration while the op amps with a higher supply had a 10 μ s longer duration. The majority of the SETs with $V_S = \pm 5V$ had widths <10 μ s and the longest ones lasted <50 μ s and the majority of the SETs on the op amps with a $V_S = \pm 15V$ had widths <20 μ s and the longest ones lasted <60 μ s. The increase in time is just due to the fact that op amps biased at $\pm 15V$ experienced a larger deviation and since the slew rate does not vary with supply voltage, it takes longer to recover.

Simply stating that an SET could last as long as 50 μ s or 60 μ s, depending on the supply voltage does not give a true indication of the performance of the part. The need for further analysis arises from the distribution of the duration of the events.

Figure 17 is the histogram plot of channel B transient duration for run 421 at an LET = 28.0MeV · cm²/mg and a supply voltage of $\pm 5V$. The distribution is bimodal, with the majority of the transient widths being 10-20 μ s (data set A) in duration and a few number of transients recovering in the 40-50 μ s range (data set B). Data set A has a total of 564 counts and a cross section of 2.82×10^{-4} cm². Data set B has a total of 35 counts and a cross section of 1.75×10^{-5} cm². The cross section for transients lasting in the 40-50 μ s range is over a magnitude lower than those in the 10-20 μ s range and the probability of an SET (which falls under data set B) occurring is much lower than that of data set A. In addition, since the length of the duration does not vary with LET level, the same bimodal distribution will occur at all LET levels.

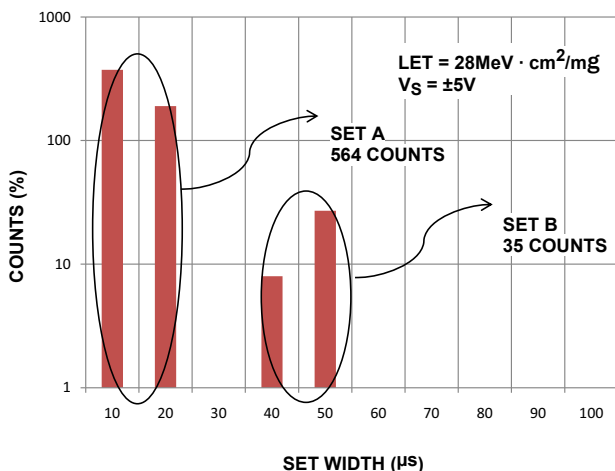


FIGURE 17. RUN 421 CHANNEL B SET WIDTH HISTOGRAM PLOT

Figure 18 is the histogram plot of channel A transient duration for run 422 at an LET = 28.0MeV · cm²/mg and a supply voltage of $\pm 15V$. The distribution is also bimodal, with the majority of the transient widths being 10-20 μ s (data set A) in duration and a few number of transients recovering in the 50-60 μ s range (data set B). Data set A has a total of 409 counts and a cross section of 2.05×10^{-4} cm². Data set B has a total of 23 counts and a cross section of 1.15×10^{-5} cm². This demonstrates that even though the ISL70417SEH experiences SETs that prolong in the 50 μ s-60 μ s range, the cross section for those events are a magnitude lower than those that last between 10 and 20 μ s.

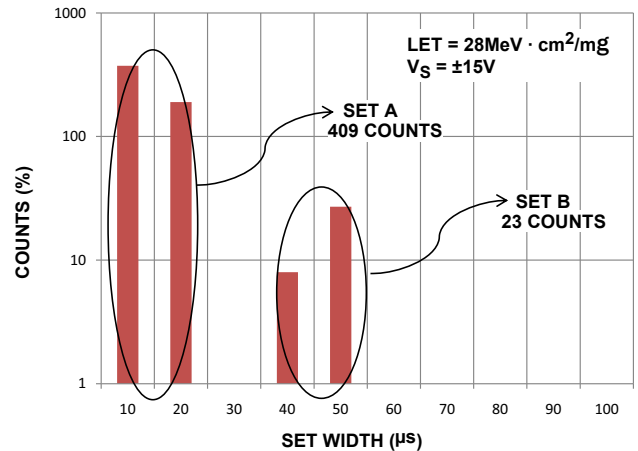


FIGURE 18. RUN 422 CHANNEL A SET WIDTH HISTOGRAM PLOT

In addition, the bimodal distribution clearly indicates there are different areas of sensitivity and so supports the interpretation of distinct cross sections from truly different physical mechanisms. A summary of the bimodal distribution and cross section is shown below:

DATA SET	V_S	LET	CROSS SECTION
A	$\pm 5V$	LET = 28MeV · cm ² /mg	2.82×10^{-4} cm ²
B	$\pm 5V$	LET = 28MeV · cm ² /mg	1.75×10^{-5} cm ²
A	$\pm 15V$	LET = 28MeV · cm ² /mg	2.05×10^{-4} cm ²
B	$\pm 15V$	LET = 28MeV · cm ² /mg	1.15×10^{-5} cm ²

Figures 19 through 58 represent transients on each channel of the amplifier under various LET values and both bias conditions. The plots are a composite of the first 50 transients captured on the scope. This information is useful in quantifying the excursion of the output as a result of SEE induced transients.

Typical SET Captures

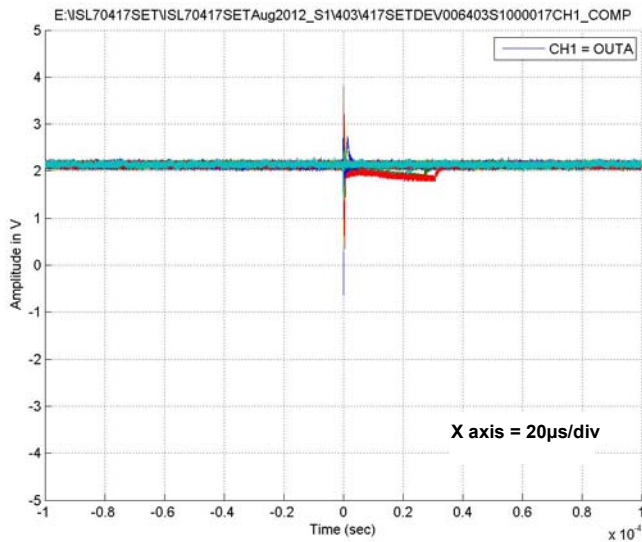


FIGURE 19. TYPICAL CAPTURE AT $V_S = \pm 5V$, CHANNEL A,
LET = $2.7MeV \cdot cm^2/mg$, RUN 403

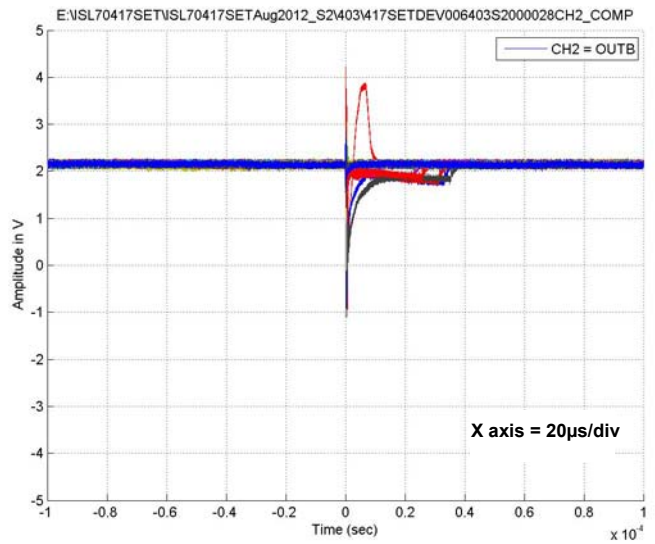


FIGURE 20. TYPICAL CAPTURE AT $V_S = \pm 5V$, CHANNEL B,
LET = $2.7MeV \cdot cm^2/mg$, RUN 403

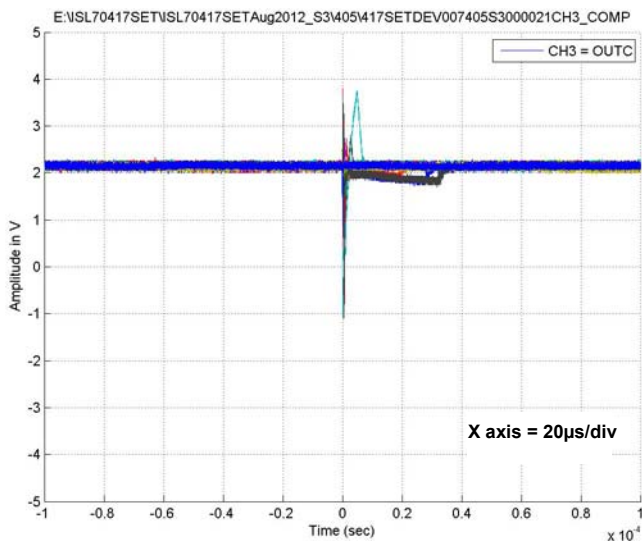


FIGURE 21. TYPICAL CAPTURE AT $V_S = \pm 5V$, CHANNEL C,
LET = $2.7MeV \cdot cm^2/mg$, RUN 405

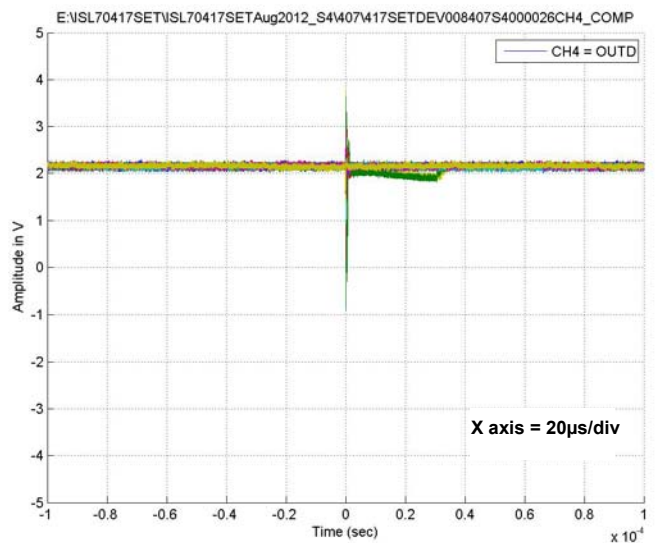


FIGURE 22. TYPICAL CAPTURE AT $V_S = \pm 5V$, CHANNEL D,
LET = $2.7MeV \cdot cm^2/mg$, RUN 407

Typical SET Captures (Continued)

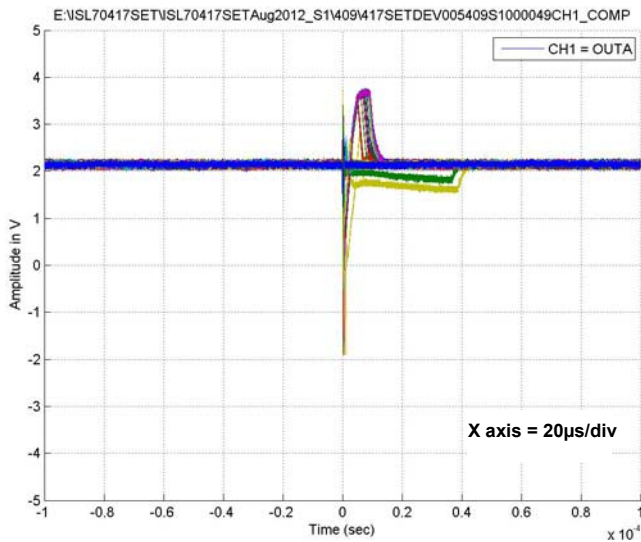


FIGURE 23. TYPICAL CAPTURE AT $V_S = \pm 5V$, CHANNEL A,
LET = $8.5MeV \cdot cm^2/mg$, RUN 409

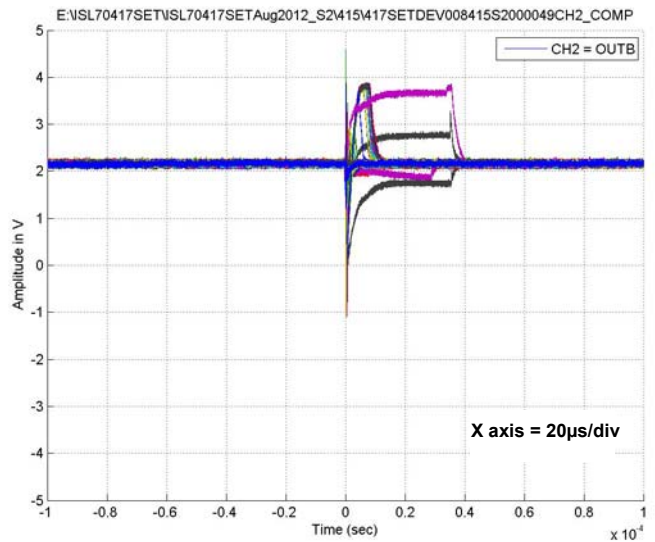


FIGURE 24. TYPICAL CAPTURE AT $V_S = \pm 5V$, CHANNEL B,
LET = $8.5MeV \cdot cm^2/mg$, RUN 415

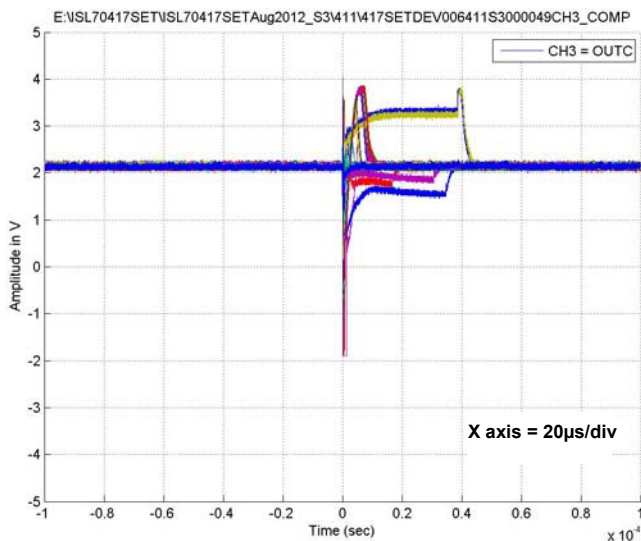


FIGURE 25. TYPICAL CAPTURE AT $V_S = \pm 5V$, CHANNEL C,
LET = $8.5MeV \cdot cm^2/mg$, RUN 411

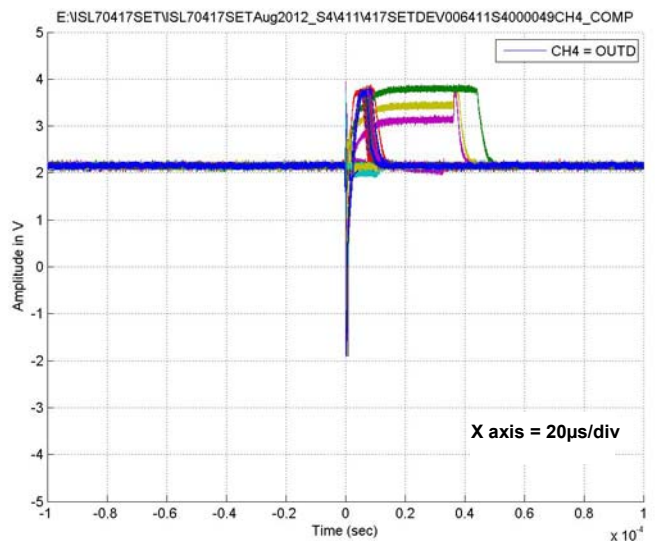


FIGURE 26. TYPICAL CAPTURE AT $V_S = \pm 5V$, CHANNEL D,
LET = $8.5MeV \cdot cm^2/mg$, RUN 411

Typical SET Captures (Continued)

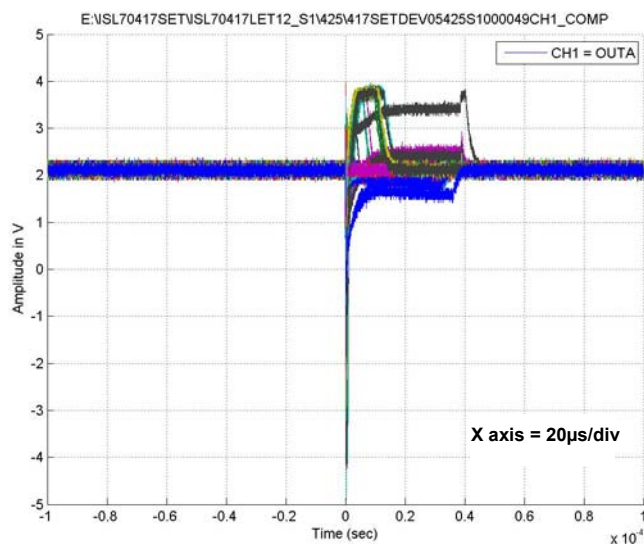


FIGURE 27. TYPICAL CAPTURE AT $V_S = \pm 5V$, CHANNEL A,
LET = $12MeV \cdot cm^2/mg$, RUN 425

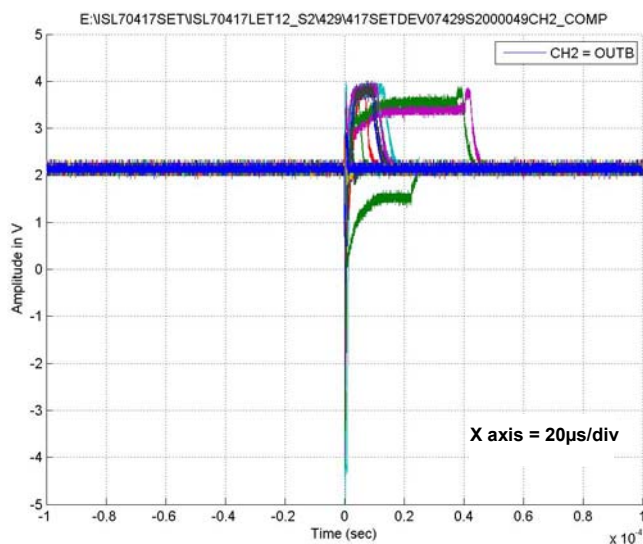


FIGURE 28. TYPICAL CAPTURE AT $V_S = \pm 5V$, CHANNEL B,
LET = $12MeV \cdot cm^2/mg$, RUN 429

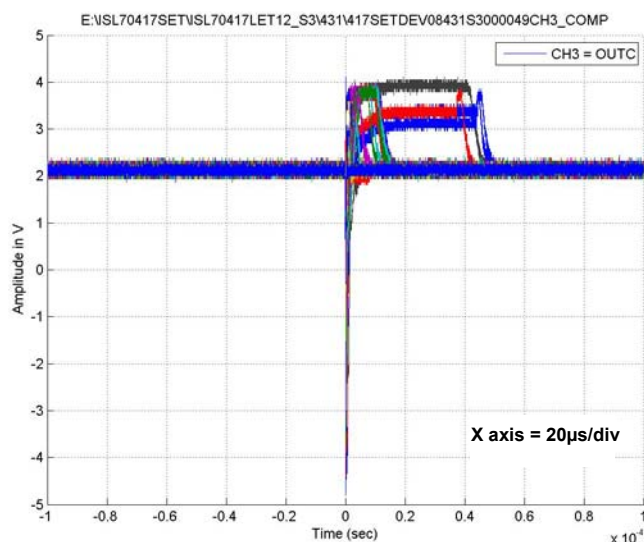


FIGURE 29. TYPICAL CAPTURE AT $V_S = \pm 5V$, CHANNEL C,
LET = $12MeV \cdot cm^2/mg$, RUN 431

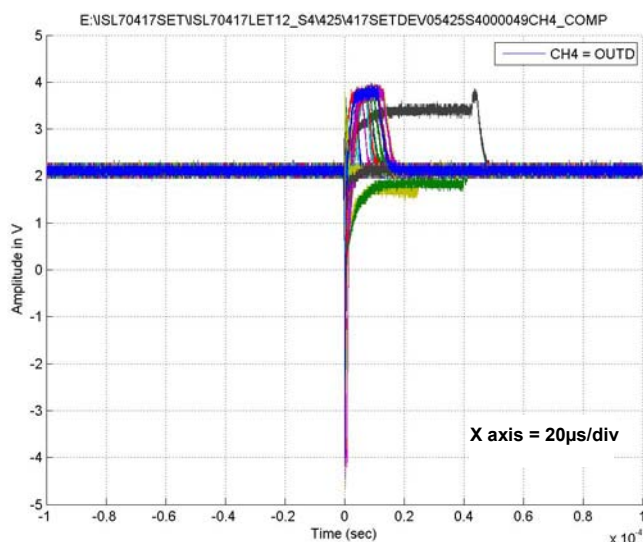


FIGURE 30. TYPICAL CAPTURE AT $V_S = \pm 5V$, CHANNEL D,
LET = $12MeV \cdot cm^2/mg$, RUN 425

Typical SET Captures (Continued)

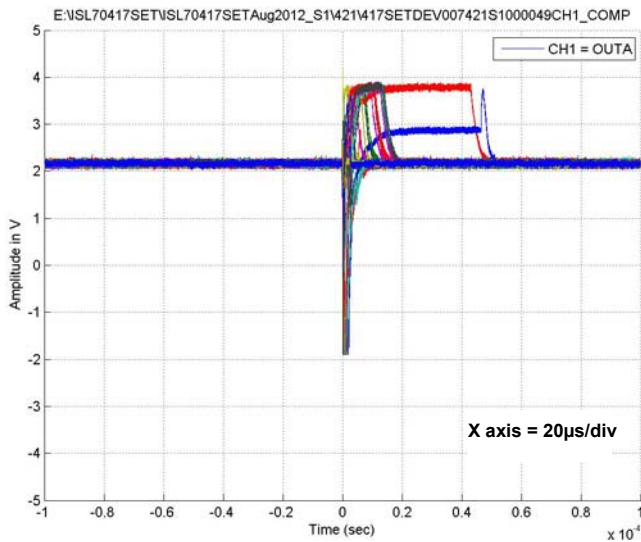


FIGURE 31. TYPICAL CAPTURE AT $V_S = \pm 5V$, CHANNEL A,
LET = 28MeV*cm²/mg², RUN 421

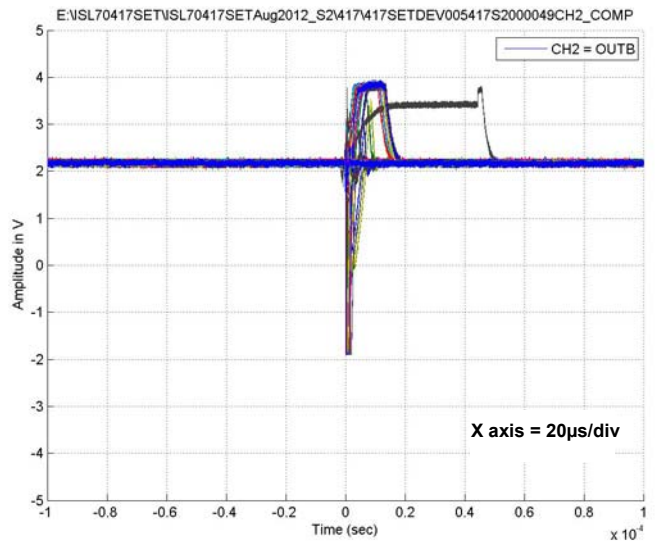


FIGURE 32. TYPICAL CAPTURE AT $V_S = \pm 5V$, CHANNEL B,
LET = 28MeV*cm²/mg, RUN 417

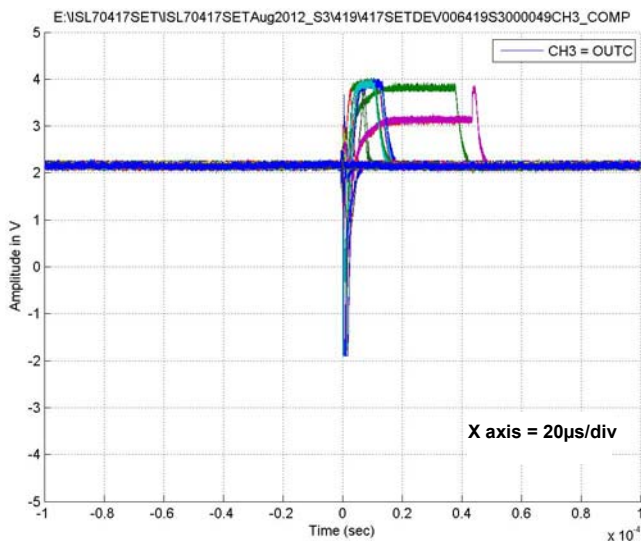


FIGURE 33. TYPICAL CAPTURE AT $V_S = \pm 5V$, CHANNEL C,
LET = 28MeV*cm²/mg, RUN 419

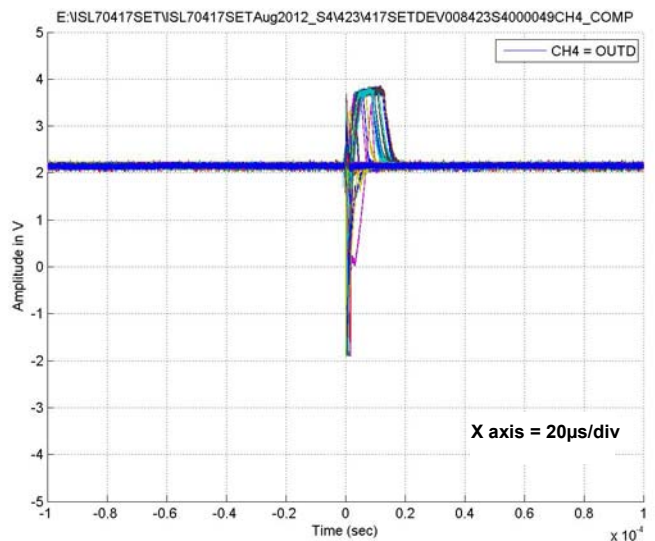


FIGURE 34. TYPICAL CAPTURE AT $V_S = \pm 5V$, CHANNEL D,
LET = 28MeV*cm²/mg, RUN 423

Typical SET Captures (Continued)

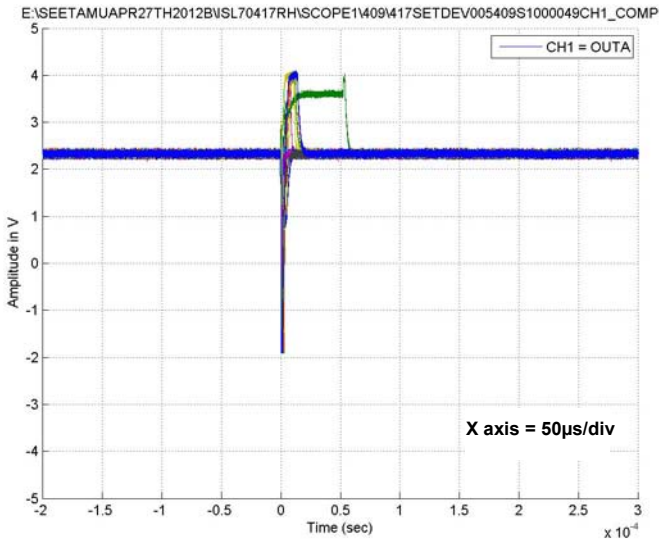


FIGURE 35. TYPICAL CAPTURE AT $V_S = \pm 5V$, CHANNEL A,
LET = $44MeV \cdot cm^2/mg$, RUN 409

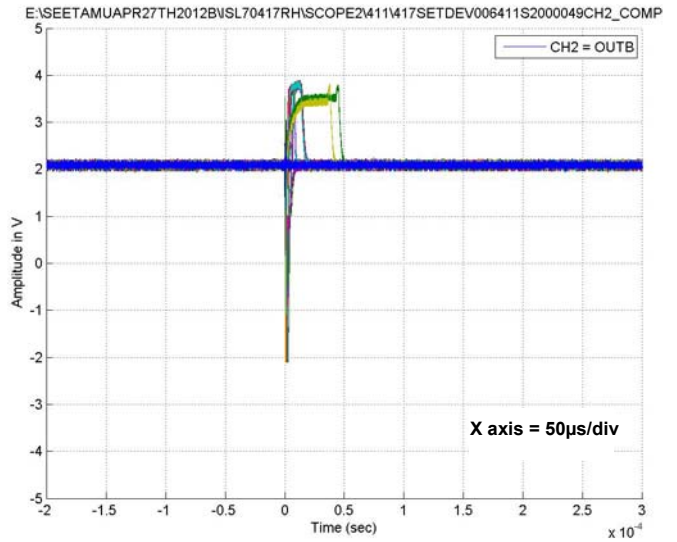


FIGURE 36. TYPICAL CAPTURE AT $V_S = \pm 5V$, CHANNEL B,
LET = $44MeV \cdot cm^2/mg$, RUN 411

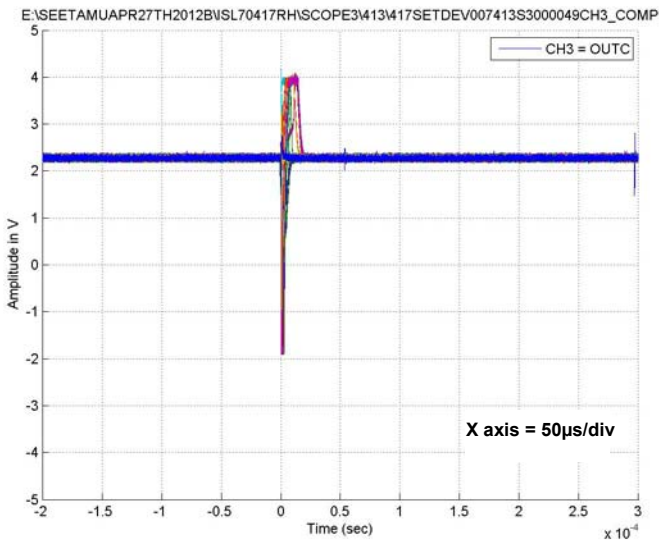


FIGURE 37. TYPICAL CAPTURE AT $V_S = \pm 5V$, CHANNEL C,
LET = $44MeV \cdot cm^2/mg$, RUN 413

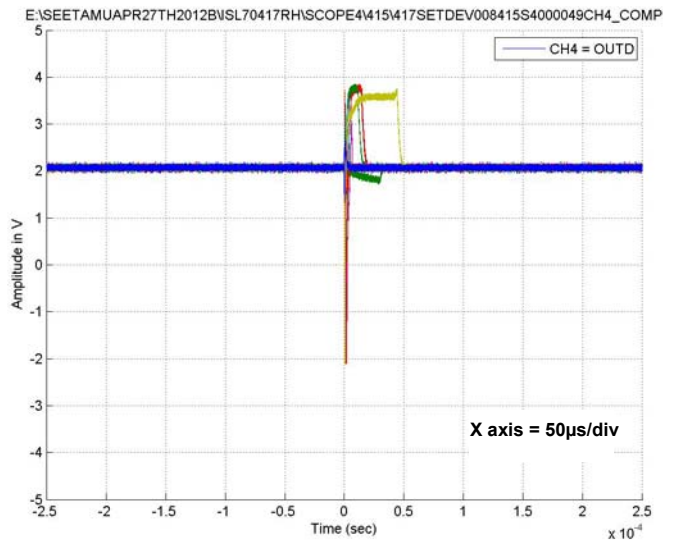


FIGURE 38. TYPICAL CAPTURE AT $V_S = \pm 5V$, CHANNEL D,
LET = $44MeV \cdot cm^2/mg$, RUN 415

Typical SET Captures (Continued)

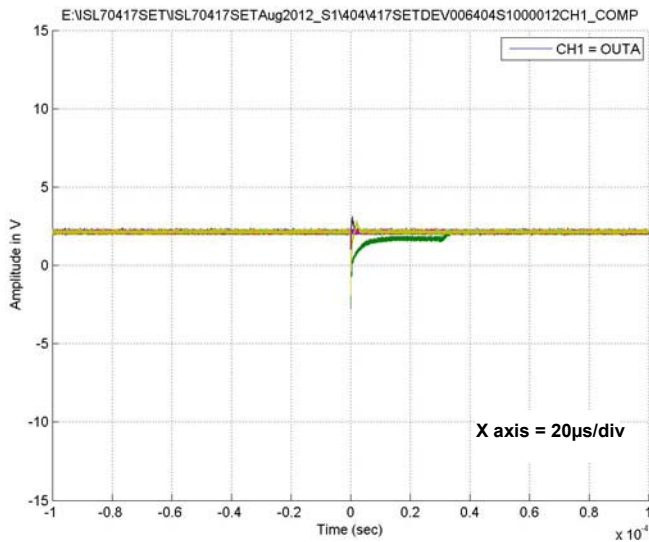


FIGURE 39. TYPICAL CAPTURE AT $V_S = \pm 15V$, CHANNEL A,
LET = $2.7MeV \cdot cm^2/mg$, RUN 404

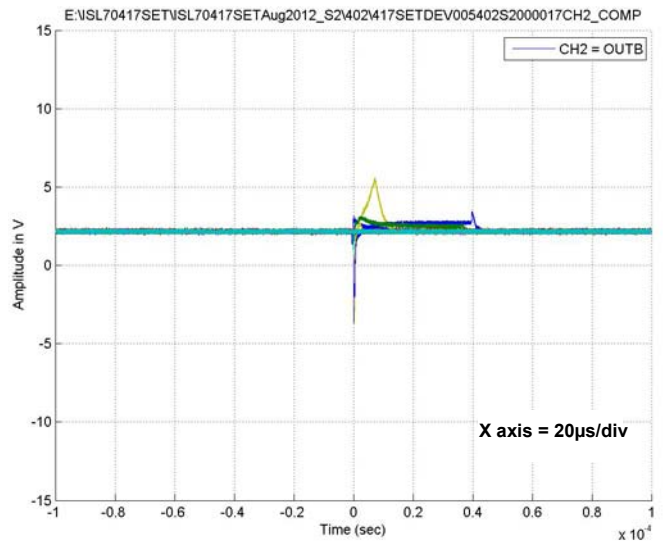


FIGURE 40. TYPICAL CAPTURE AT $V_S = \pm 15V$, CHANNEL B,
LET = $2.7MeV \cdot cm^2/mg$, RUN 402

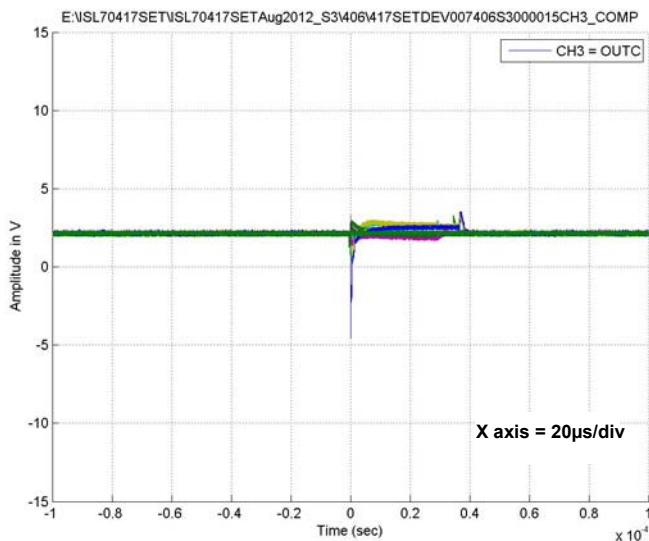


FIGURE 41. TYPICAL CAPTURE AT $V_S = \pm 15V$, CHANNEL C,
LET = $2.7MeV \cdot cm^2/mg$, RUN 406

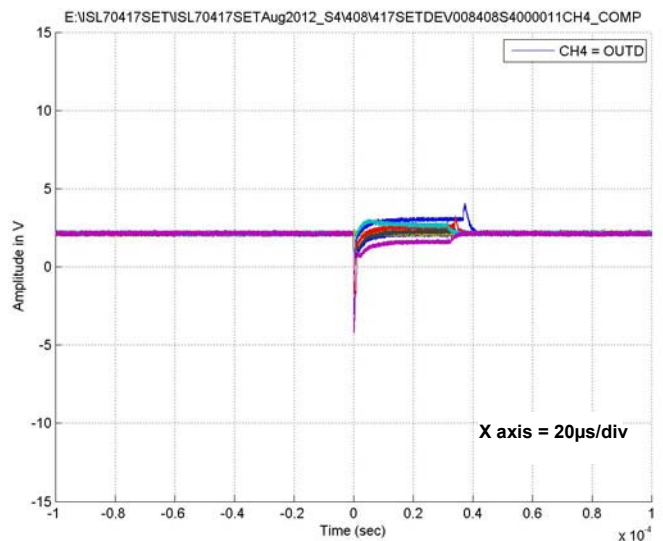


FIGURE 42. TYPICAL CAPTURE AT $V_S = \pm 15V$, CHANNEL D,
LET = $2.7MeV \cdot cm^2/mg$, RUN 408

Typical SET Captures (Continued)

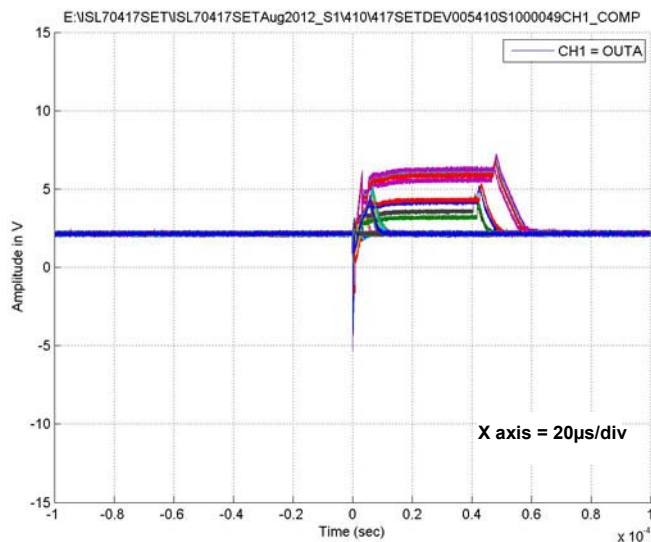


FIGURE 43. TYPICAL CAPTURE AT $V_S = \pm 15V$, CHANNEL A,
LET = $8.5MeV \cdot cm^2/mg$, RUN 410

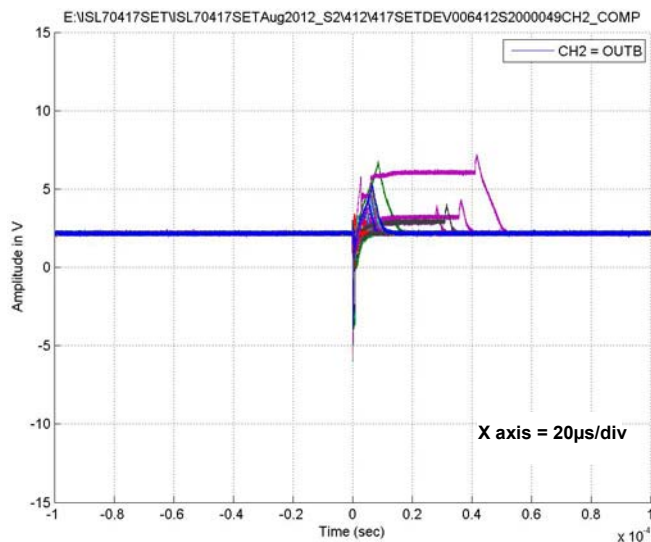


FIGURE 44. TYPICAL CAPTURE AT $V_S = \pm 15V$, CHANNEL B,
LET = $8.5MeV \cdot cm^2/mg$, RUN 412

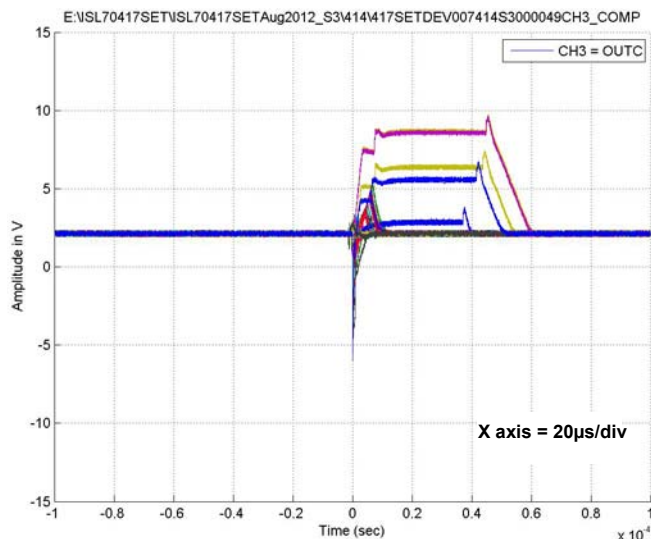


FIGURE 45. TYPICAL CAPTURE AT $V_S = \pm 15V$, CHANNEL C,
LET = $8.5MeV \cdot cm^2/mg$, RUN 414

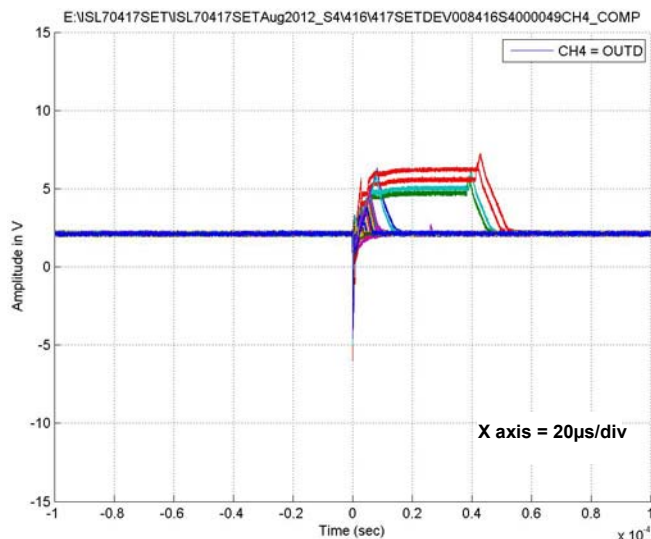


FIGURE 46. TYPICAL CAPTURE AT $V_S = \pm 15V$, CHANNEL D,
LET = $8.5MeV \cdot cm^2/mg$, RUN 416

Typical SET Captures (Continued)

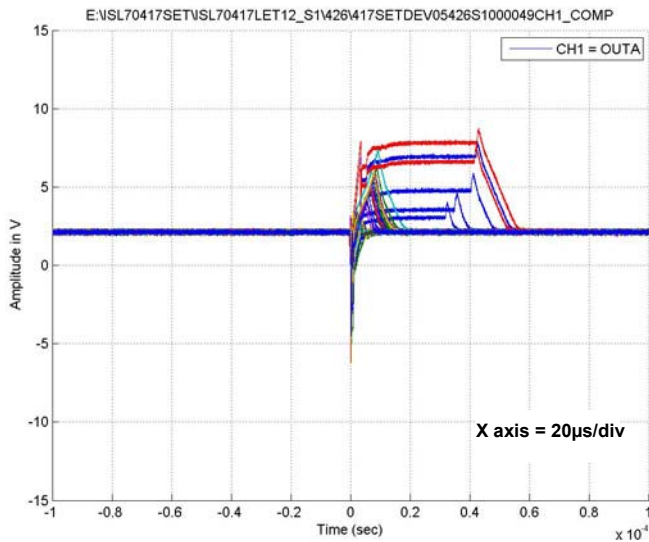


FIGURE 47. TYPICAL CAPTURE AT $V_S = \pm 15V$, CHANNEL A,
LET = $12MeV \cdot cm^2/mg$, RUN 426

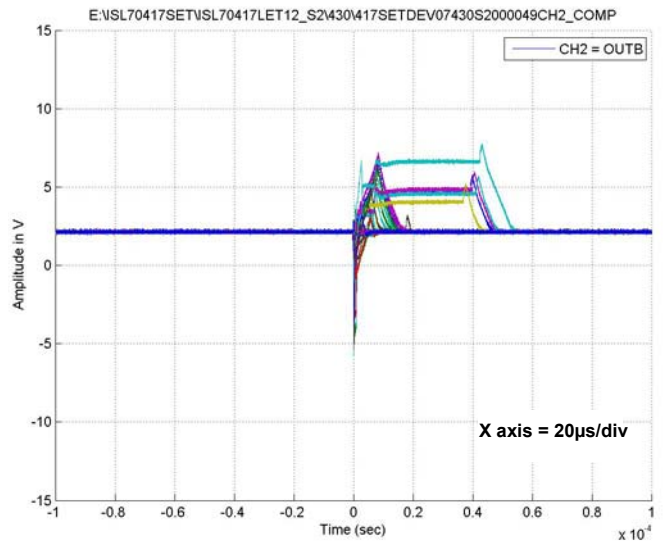


FIGURE 48. TYPICAL CAPTURE AT $V_S = \pm 15V$, CHANNEL B,
LET = $12MeV \cdot cm^2/mg$, RUN 430

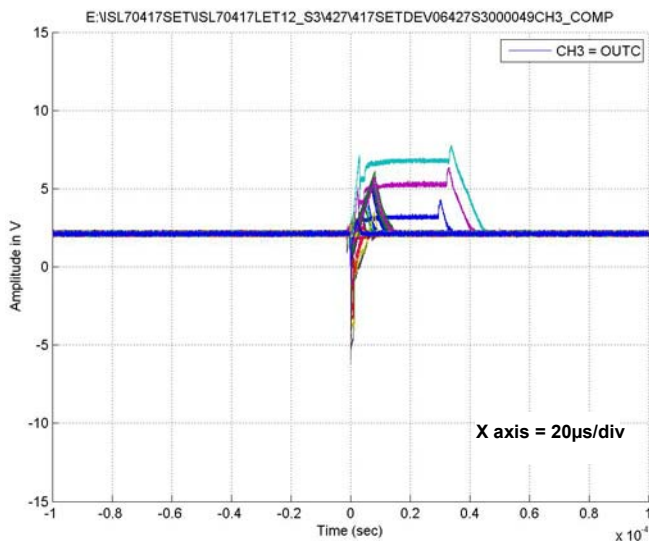


FIGURE 49. TYPICAL CAPTURE AT $V_S = \pm 15V$, CHANNEL C,
LET = $12MeV \cdot cm^2/mg$, RUN 427

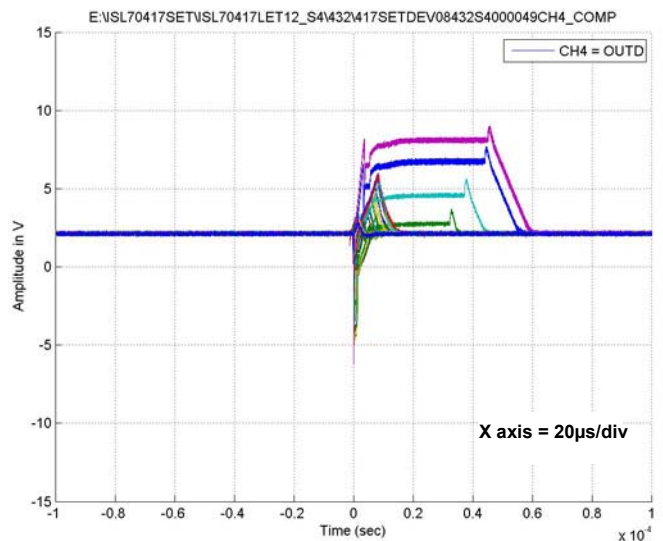


FIGURE 50. TYPICAL CAPTURE AT $V_S = \pm 15V$, CHANNEL D,
LET = $12MeV \cdot cm^2/mg$, RUN 432

Typical SET Captures (Continued)

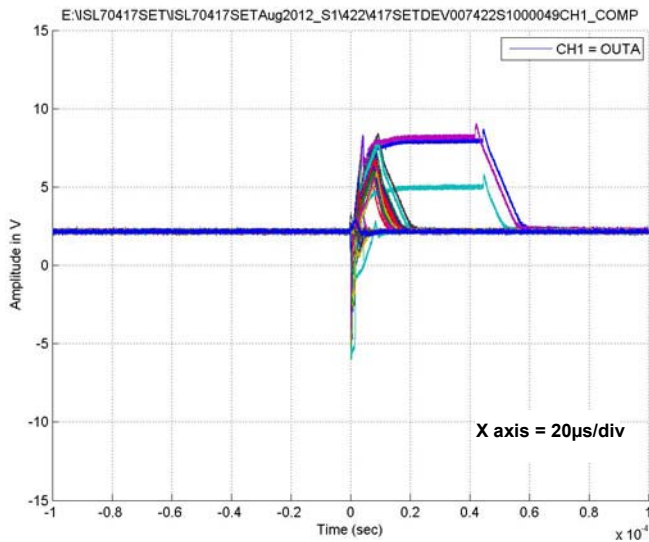


FIGURE 51. TYPICAL CAPTURE AT $V_S = \pm 15V$, CHANNEL A,
LET = 28MeV*cm²/mg², RUN 422

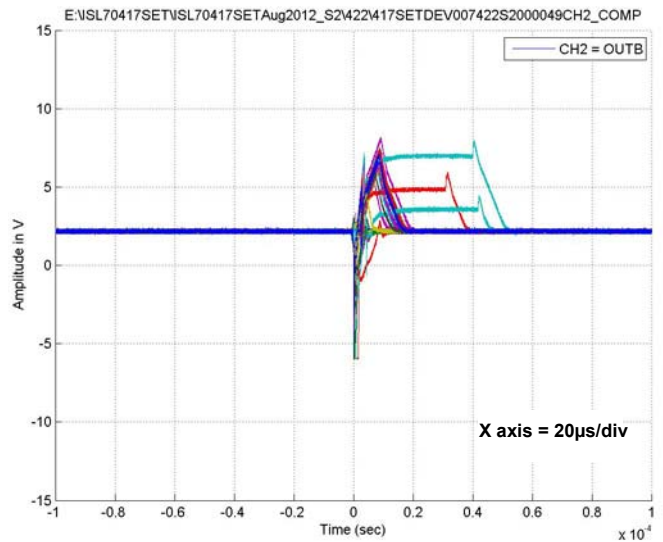


FIGURE 52. TYPICAL CAPTURE AT $V_S = \pm 15V$, CHANNEL B,
LET = 28MeV*cm²/mg, RUN 422

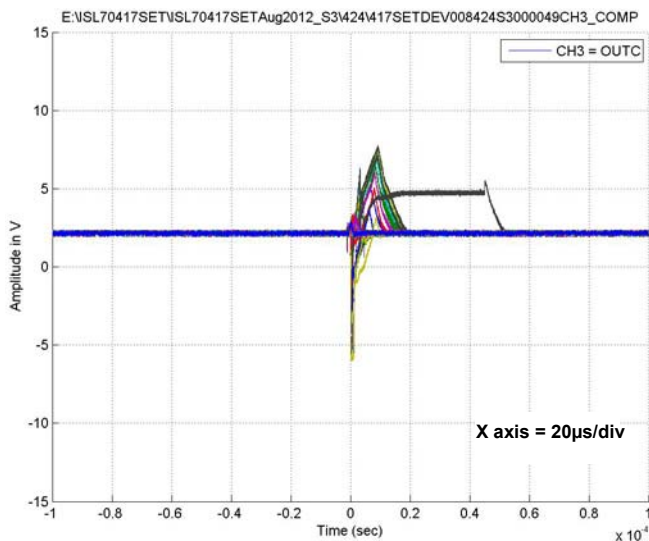


FIGURE 53. TYPICAL CAPTURE AT $V_S = \pm 15V$, CHANNEL C,
LET = 28MeV*cm²/mg, RUN 424

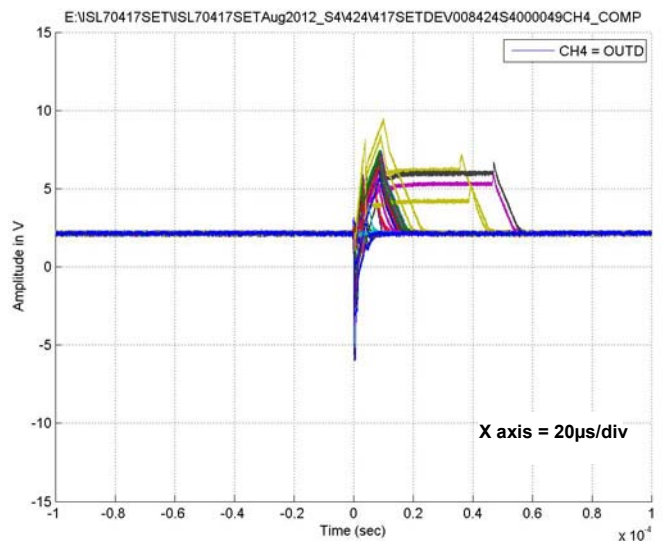


FIGURE 54. TYPICAL CAPTURE AT $V_S = \pm 15V$, CHANNEL D,
LET = 28MeV*cm²/mg, RUN 424

Typical SET Captures (Continued)

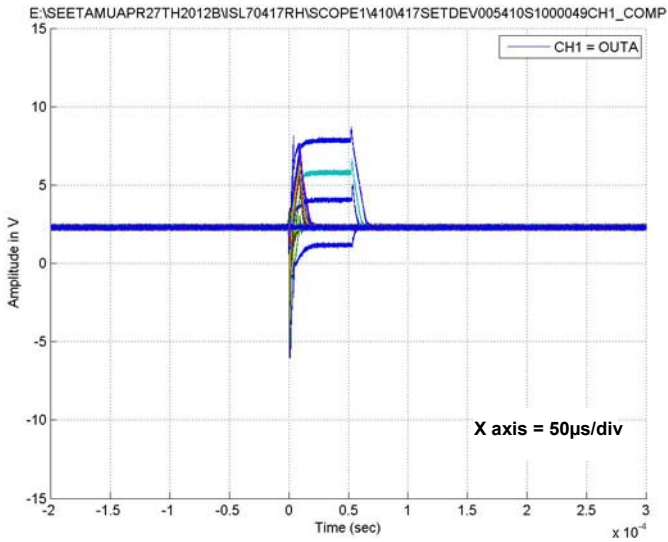


FIGURE 55. TYPICAL CAPTURE AT $V_S = \pm 15V$, CHANNEL A,
LET = 44MeV*cm²/mg, RUN 410

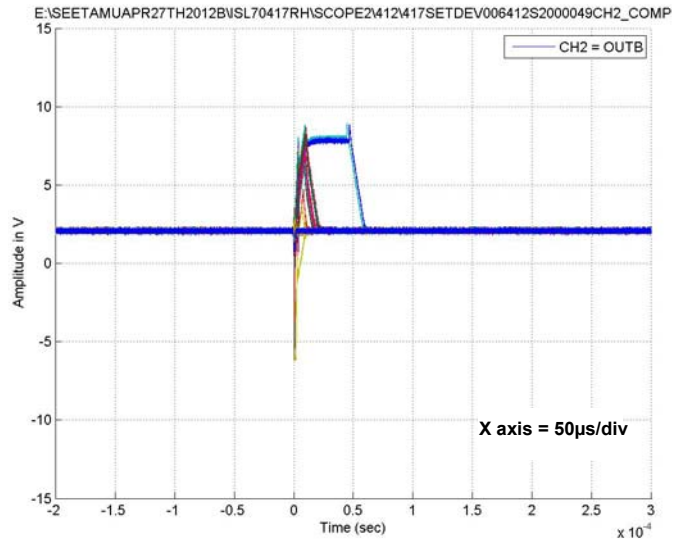


FIGURE 56. TYPICAL CAPTURE AT $V_S = \pm 15V$, CHANNEL B,
LET = 44MeV*cm²/mg, RUN 412

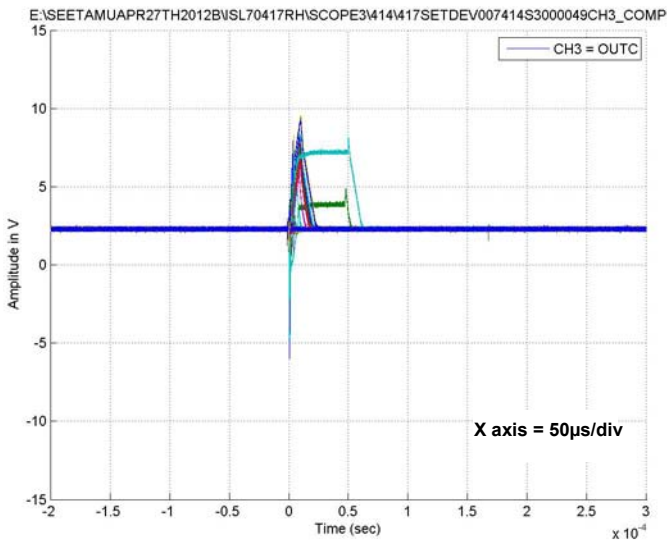


FIGURE 57. TYPICAL CAPTURE AT $V_S = \pm 15V$, CHANNEL C,
LET = 44MeV*cm²/mg, RUN 414

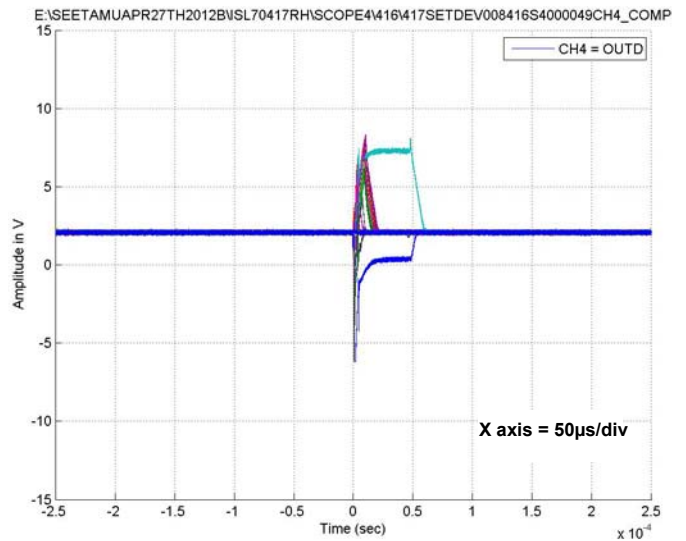


FIGURE 58. TYPICAL CAPTURE AT $V_S = \pm 15V$, CHANNEL D,
LET = 44MeV*cm²/mg, RUN 416

Summary

Single Event Burnout

No single event burnout (SEB) was observed for the device up to an LET of $73.9\text{MeV} \cdot \text{cm}^2/\text{mg}$ ($+125^\circ\text{C}$) at a maximum voltage supply of $V_S = \pm 20\text{V}$. SEB was tested and passed at a supply voltage $V_S = \pm 20\text{V}$. This gives over 20% margin on the recommended supply voltage of $V_S = \pm 15\text{V}$. Since the operational amplifier has no internal ground reference, the 40V supply range can be partitioned as desired, for example have a single supply where the V^+ pin can be tied to 40V and the V^- pin tied to ground (0V).

It is also not surprising that since the process is an SOI process, there was no latch-up observed on the device.

Single Event Transient

Based on the results presented, the ISL70417SEH op amp offers advantages over one competitor's part by having a lower SET cross section at a gain of 10[1]. The length of worst case SETs can be $50\mu\text{s}$ for devices with $V_S = \pm 5\text{V}$ and $60\mu\text{s}$ for devices with $V_S = \pm 15\text{V}$. However, it has been demonstrated that the cross section of the events that last in the $50\text{-}60\mu\text{s}$ range is a magnitude lower than those lasting $10\text{-}20\mu\text{s}$. This part does not experience the long recovery time ($>100\mu\text{s}$) during a single event transient seen on other competitor op amps in a comparator application[2]. This may be explained by the higher drive capability of the ISL70417SEH and its ability to drive highly capacitive loads. Magnitude of the deviation for $V_S = \pm 5\text{V}$ was to 1V below the rail in the positive direction and 2V above the rail in the negative direction. For amplifiers supplied with a $V_S = \pm 15\text{V}$, the transient excursions were much larger, however they do not extend to the expected VOH or VOL levels of $\pm 13.5\text{V}$. All the transients observed were 8.5V deviations or less and recovery time of the transients were less than $60\mu\text{s}$. Figures 59 and 60 show the histogram of the voltage deviation magnitude during a SET. These results are from run 410, the ISL70417SEH was biased with a $V_S = \pm 15\text{V}$ and an LET of $44\text{MeV} \cdot \text{cm}^2/\text{mg}$ was used during the run. This demonstrates the peak magnitude the output voltage deviates due to a SET at the highest tested LET.

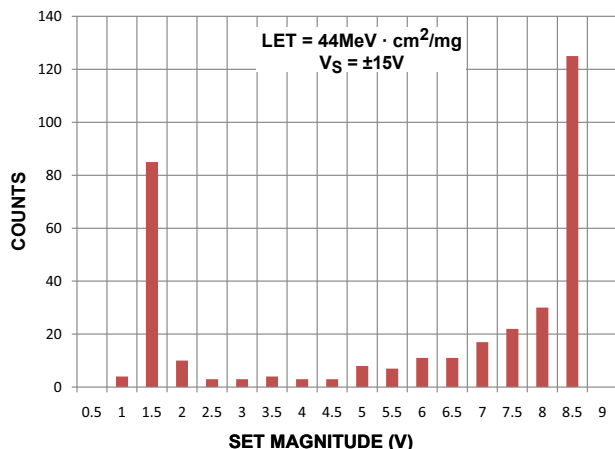


FIGURE 59. RUN 410 NEGATIVE TRANSIENT HISTOGRAM

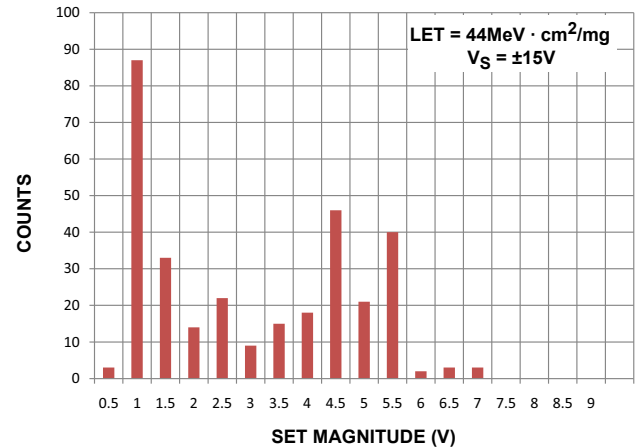


FIGURE 60. RUN 410 POSITIVE TRANSIENT HISTOGRAM

Overall, the ISL70417SEH is very well behaved in a heavy ion environment. In space flight applications, the ISL70417SEH may require filtering or other types of SET mitigation techniques. However, the ISL70417SEH offers a competitive advantage over other rad hard op amps by offering:

- No single event burnout up to $\pm 40\text{V}$
- SOI process for latch-up immunity
- Very low cross section for significant SETs:
 - $V_S = \pm 5\text{V}$: $1.75 \times 10^{-5} \text{cm}^2$
 - $V_S = \pm 15\text{V}$: $1.15 \times 10^{-5} \text{cm}^2$
- A lower cross section at similar gain and LET than its major competitor

References

- [1] Ray Ladbury and Stephen Buchner, "SEE Testing of the RH1013 Dual Precision Operational Amplifier" http://radhome.gsfc.nasa.gov/radhome/papers/T121805_RH1013.pdf
- [2] S. Larsson and S. Mattsson, "Heavy Ion Transients in Operational Amplifier of Type LM124, RH1014 and OP27" <https://escies.org/download/webDocumentFile?id=837>

Appendix A

Appendix A includes the data from Figures 3 through 10 in tabular format, complete test schematic, and top silk screen image.

TABLE 3. DATA OF CHANNEL CROSS SECTION OF THE ISL70417SEH REPRESENTED IN FIGURES 3 THROUGH 6

SUPPLY VOLTAGE (V)	LET (MeV . cm ² /mg)	CHANNEL	NUMBER OF RUNS	FLUENCE PER RUN (PARTICLES/cm ²)	EVENTS	EVENT CS (cm ²)	90% CI UPPER LIMIT (cm ²)	90% CI LOWER LIMIT (cm ²)
±5	±5	A	4	2.0 x 10 ⁶	74	9.25 x 10 ⁻⁶	1.12 x 10 ⁻⁵	7.59 x 10 ⁻⁶
±5	8.5	A	4	2.0 x 10 ⁶	868	1.09 x 10 ⁻⁴	1.14 x 10 ⁻⁴	1.02 x 10 ⁻⁴
±5	12	A	4	2.0 x 10 ⁶	1023	1.28 x 10 ⁻⁴	1.34 x 10 ⁻⁴	1.21 x 10 ⁻⁴
±5	28	A	4	2.0 x 10 ⁶	2253	2.82 x 10 ⁻⁴	2.90 x 10 ⁻⁴	2.70 x 10 ⁻⁴
±5	44	A	4	1.0 x 10 ⁶	2042	5.11 x 10 ⁻⁴	5.26 x 10 ⁻⁴	4.90 x 10 ⁻⁴
±5	2.7	B	4	2.0 x 10 ⁶	105	1.31 x 10 ⁻⁵	1.54 x 10 ⁻⁵	1.12 x 10 ⁻⁵
±5	8.5	B	4	2.0 x 10 ⁶	921	1.15 x 10 ⁻⁴	1.21 x 10 ⁻⁴	1.08 x 10 ⁻⁴
±5	12	B	4	2.0 x 10 ⁶	1049	1.31 x 10 ⁻⁴	1.38 x 10 ⁻⁴	1.25 x 10 ⁻⁴
±5	28	B	4	2.0 x 10 ⁶	2599	3.25 x 10 ⁻⁴	3.35 x 10 ⁻⁴	3.12 x 10 ⁻⁴
±5	44	B	4	1.0 x 10 ⁶	2641	6.60 x 10 ⁻⁴	6.80 x 10 ⁻⁴	6.34 x 10 ⁻⁴
±5	2.7	C	4	2.0 x 10 ⁶	95	1.19 x 10 ⁻⁵	1.40 x 10 ⁻⁵	9.98 x 10 ⁻⁶
±5	8.5	C	4	2.0 x 10 ⁶	1016	1.27 x 10 ⁻⁴	1.33 x 10 ⁻⁴	1.19 x 10 ⁻⁴
±5	12	C	4	2.0 x 10 ⁶	1139	1.42 x 10 ⁻⁴	1.49 x 10 ⁻⁴	1.35 x 10 ⁻⁴
±5	28	C	4	2.0 x 10 ⁶	3197	4.00 x 10 ⁻⁴	4.08 x 10 ⁻⁴	3.88 x 10 ⁻⁴
±5	44	C	4	1.0 x 10 ⁶	2610	6.53 x 10 ⁻⁴	6.72 x 10 ⁻⁴	6.26 x 10 ⁻⁴
±5	2.7	D	4	2.0 x 10 ⁶	118	1.48 x 10 ⁻⁵	1.71 x 10 ⁻⁵	1.27 x 10 ⁻⁵
±5	8.5	D	4	2.0 x 10 ⁶	1002	1.25 x 10 ⁻⁴	1.32 x 10 ⁻⁴	1.18 x 10 ⁻⁴
±5	12	D	4	2.0 x 10 ⁶	1113	1.39 x 10 ⁻⁴	1.46 x 10 ⁻⁴	1.32 x 10 ⁻⁴
±5	28	D	4	2.0 x 10 ⁶	2560	3.20 x 10 ⁻⁴	3.30 x 10 ⁻⁴	3.07 x 10 ⁻⁴
±5	44	D	4	1.0 x 10 ⁶	1509	3.77 x 10 ⁻⁴	3.92 x 10 ⁻⁴	3.58 x 10 ⁻⁴

Single Event Effects Testing of the ISL70417SEH,
Quad 40V Rad Hard Precision Operation Amplifiers

TABLE 4. DATA OF CHANNEL CROSS SECTION OF THE ISL70417SEH REPRESENTED IN FIGURES 3 THROUGH 6

SUPPLY VOLTAGE (V)	LET (MeV · cm ² /mg)	CHANNEL	NUMBER OF RUNS	FLUENCE PER RUN (PARTICLES/cm ²)	EVENTS	EVENT CS (cm ²)	90% CI UPPER LIMIT (cm ²)	90% CI LOWER LIMIT (cm ²)
±15	2.7	A	4	2.0 x 10 ⁶	68	8.50 x 10 ⁻⁶	1.04E-05	6.97 x 10 ⁻⁶
±15	8.5	A	4	2.0 x 10 ⁶	599	7.49 x 10 ⁻⁵	7.94 x 10 ⁻⁵	6.96 x 10 ⁻⁵
±15	12	A	4	2.0 x 10 ⁶	909	1.14 x 10 ⁻⁴	1.19 x 10 ⁻⁴	1.07 x 10 ⁻⁴
±15	28	A	4	2.0 x 10 ⁶	1909	2.39 x 10 ⁻⁴	2.46 x 10 ⁻⁴	2.29 x 10 ⁻⁴
±15	44	A	4	1.0 x 10 ⁶	1777	4.44 x 10 ⁻⁴	4.58 x 10 ⁻⁴	4.26 x 10 ⁻⁴
±15	2.7	B	4	2.0 x 10 ⁶	50	6.25 x 10 ⁻⁶	7.87 x 10 ⁻⁶	4.94 x 10 ⁻⁶
±15	8.5	B	4	2.0 x 10 ⁶	795	9.94 x 10 ⁻⁵	1.05 x 10 ⁻⁴	9.34 x 10 ⁻⁵
±15	12	B	4	2.0 x 10 ⁶	946	1.18 x 10 ⁻⁴	1.24 x 10 ⁻⁴	1.11 x 10 ⁻⁴
±15	28	B	4	2.0 x 10 ⁶	2010	2.51 x 10 ⁻⁴	2.59 x 10 ⁻⁴	2.41 x 10 ⁻⁴
±15	44	B	4	1.0 x 10 ⁶	2056	5.14 x 10 ⁻⁴	5.29 x 10 ⁻⁴	4.93 x 10 ⁻⁴
±15	2.7	C	4	2.0 x 10 ⁶	63	7.88 x 10 ⁻⁶	9.69 x 10 ⁻⁶	6.38 x 10 ⁻⁶
±15	8.5	C	4	2.0 x 10 ⁶	877	1.10 x 10 ⁻⁴	1.15 x 10 ⁻⁴	1.03 x 10 ⁻⁴
±15	12	C	4	2.0 x 10 ⁶	1164	1.46 x 10 ⁻⁴	1.51 x 10 ⁻⁴	1.38 x 10 ⁻⁴
±15	28	C	4	2.0 x 10 ⁶	2677	3.35 x 10 ⁻⁴	3.45 x 10 ⁻⁴	3.21 x 10 ⁻⁴
±15	44	C	4	1.0 x 10 ⁶	1574	3.94 x 10 ⁻⁴	4.09 x 10 ⁻⁴	3.74 x 10 ⁻⁴
±15	2.7	D	4	2.0 x 10 ⁶	58	7.25 x 10 ⁻⁶	8.99 x 10 ⁻⁶	5.80 x 10 ⁻⁶
±15	8.5	D	4	2.0 x 10 ⁶	686	8.58 x 10 ⁻⁵	9.09 x 10 ⁻⁵	7.97 x 10 ⁻⁵
±15	12	D	4	2.0 x 10 ⁶	1099	1.37 x 10 ⁻⁴	1.44 x 10 ⁻⁴	1.31 x 10 ⁻⁴
±15	28	D	4	2.0 x 10 ⁶	2047	2.56 x 10 ⁻⁴	2.64 x 10 ⁻⁴	2.41 x 10 ⁻⁴
±15	44	D	4	1.0 x 10 ⁶	1069	2.67 x 10 ⁻⁴	2.81 x 10 ⁻⁴	2.54 x 10 ⁻⁴

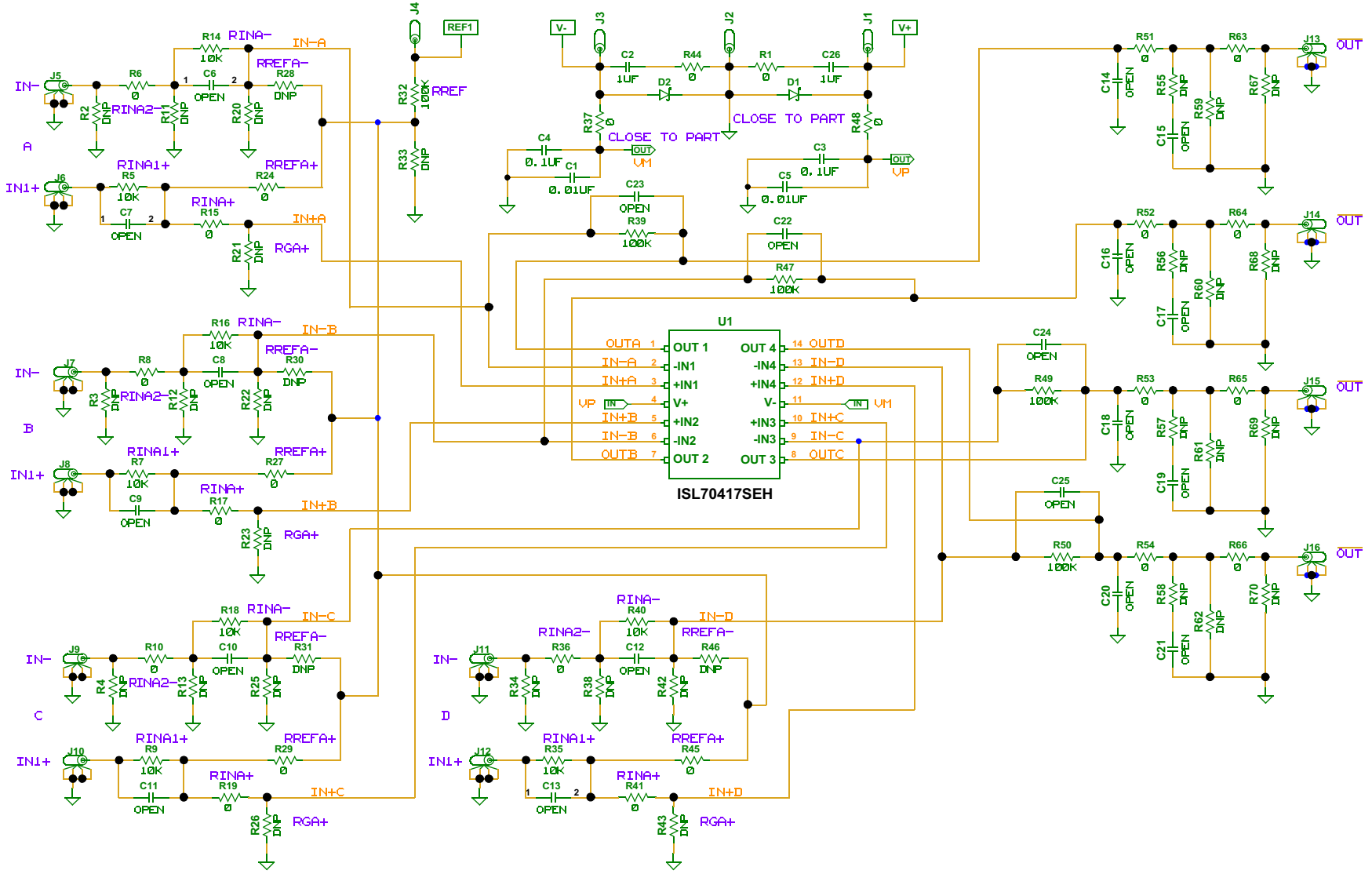
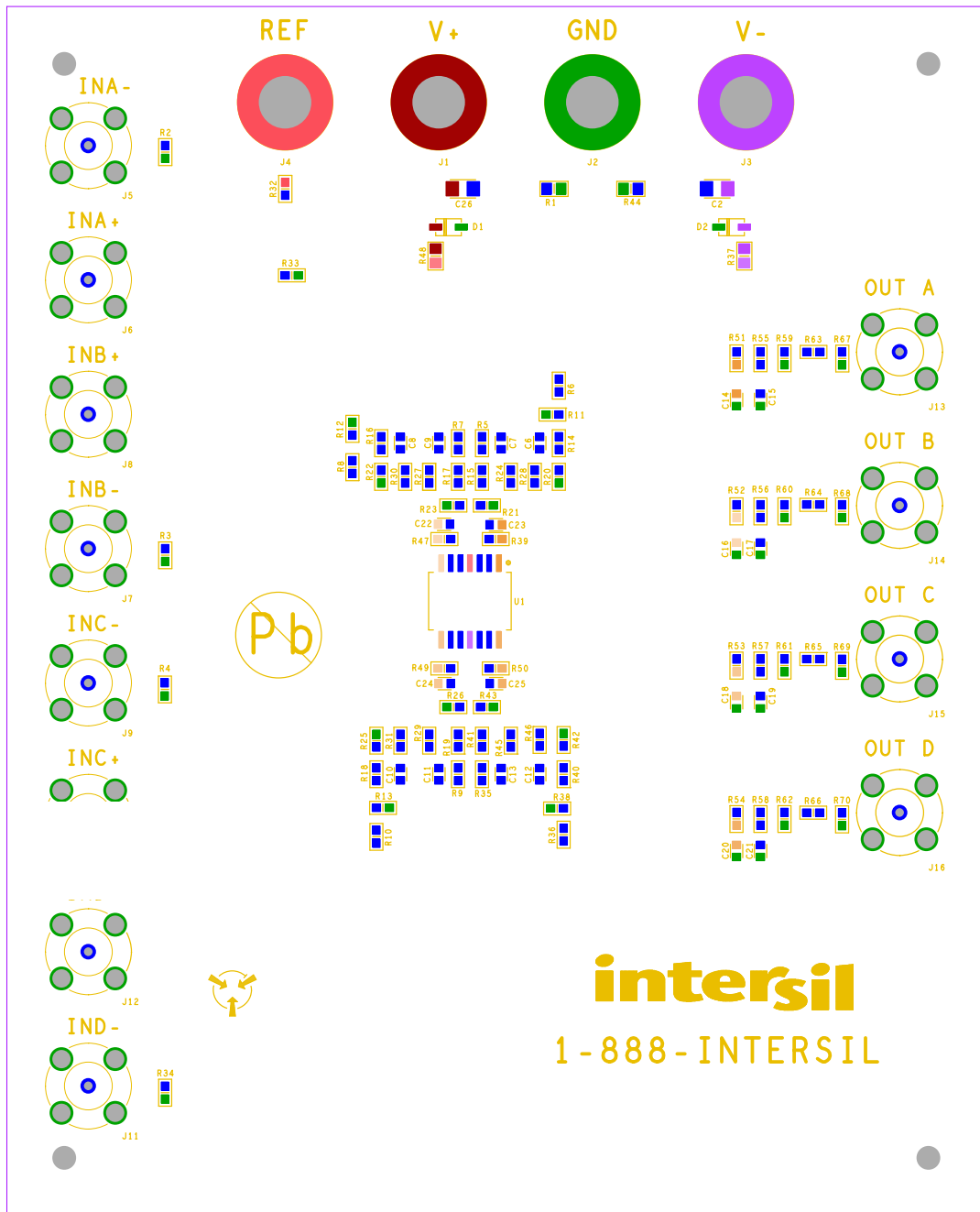


FIGURE 61. ISL70417SEH SEE TEST BOARD SCHEMATIC



SILKSCREEN TOP
INTERSIL CORPORATION

FIGURE 62. ISL70417SEH SEE TEST BOARD TOP VIEW

Notice

1. Descriptions of circuits, software and other related information in this document are provided only to illustrate the operation of semiconductor products and application examples. You are fully responsible for the incorporation or any other use of the circuits, software, and information in the design of your product or system. Renesas Electronics disclaims any and all liability for any losses and damages incurred by you or third parties arising from the use of these circuits, software, or information.
2. Renesas Electronics hereby expressly disclaims any warranties against and liability for infringement or any other claims involving patents, copyrights, or other intellectual property rights of third parties, by or arising from the use of Renesas Electronics products or technical information described in this document, including but not limited to, the product data, drawings, charts, programs, algorithms, and application examples.
3. No license, express, implied or otherwise, is granted hereby under any patents, copyrights or other intellectual property rights of Renesas Electronics or others.
4. You shall not alter, modify, copy, or reverse engineer any Renesas Electronics product, whether in whole or in part. Renesas Electronics disclaims any and all liability for any losses or damages incurred by you or third parties arising from such alteration, modification, copying or reverse engineering.
5. Renesas Electronics products are classified according to the following two quality grades: "Standard" and "High Quality". The intended applications for each Renesas Electronics product depends on the product's quality grade, as indicated below.
"Standard": Computers; office equipment; communications equipment; test and measurement equipment; audio and visual equipment; home electronic appliances; machine tools; personal electronic equipment; industrial robots; etc.
"High Quality": Transportation equipment (automobiles, trains, ships, etc.); traffic control (traffic lights); large-scale communication equipment; key financial terminal systems; safety control equipment; etc.
Unless expressly designated as a high reliability product or a product for harsh environments in a Renesas Electronics data sheet or other Renesas Electronics document, Renesas Electronics products are not intended or authorized for use in products or systems that may pose a direct threat to human life or bodily injury (artificial life support devices or systems; surgical implantations; etc.), or may cause serious property damage (space system; undersea repeaters; nuclear power control systems; aircraft control systems; key plant systems; military equipment; etc.). Renesas Electronics disclaims any and all liability for any damages or losses incurred by you or any third parties arising from the use of any Renesas Electronics product that is inconsistent with any Renesas Electronics data sheet, user's manual or other Renesas Electronics document.
6. When using Renesas Electronics products, refer to the latest product information (data sheets, user's manuals, application notes, "General Notes for Handling and Using Semiconductor Devices" in the reliability handbook, etc.), and ensure that usage conditions are within the ranges specified by Renesas Electronics with respect to maximum ratings, operating power supply voltage range, heat dissipation characteristics, installation, etc. Renesas Electronics disclaims any and all liability for any malfunctions, failure or accident arising out of the use of Renesas Electronics products outside of such specified ranges.
7. Although Renesas Electronics endeavors to improve the quality and reliability of Renesas Electronics products, semiconductor products have specific characteristics, such as the occurrence of failure at a certain rate and malfunctions under certain use conditions. Unless designated as a high reliability product or a product for harsh environments in a Renesas Electronics data sheet or other Renesas Electronics document, Renesas Electronics products are not subject to radiation resistance design. You are responsible for implementing safety measures to guard against the possibility of bodily injury, injury or damage caused by fire, and/or danger to the public in the event of a failure or malfunction of Renesas Electronics products, such as safety design for hardware and software, including but not limited to redundancy, fire control and malfunction prevention, appropriate treatment for aging degradation or any other appropriate measures. Because the evaluation of microcomputer software alone is very difficult and impractical, you are responsible for evaluating the safety of the final products or systems manufactured by you.
8. Please contact a Renesas Electronics sales office for details as to environmental matters such as the environmental compatibility of each Renesas Electronics product. You are responsible for carefully and sufficiently investigating applicable laws and regulations that regulate the inclusion or use of controlled substances, including without limitation, the EU RoHS Directive, and using Renesas Electronics products in compliance with all these applicable laws and regulations. Renesas Electronics disclaims any and all liability for damages or losses occurring as a result of your noncompliance with applicable laws and regulations.
9. Renesas Electronics products and technologies shall not be used for or incorporated into any products or systems whose manufacture, use, or sale is prohibited under any applicable domestic or foreign laws or regulations. You shall comply with any applicable export control laws and regulations promulgated and administered by the governments of any countries asserting jurisdiction over the parties or transactions.
10. It is the responsibility of the buyer or distributor of Renesas Electronics products, or any other party who distributes, disposes of, or otherwise sells or transfers the product to a third party, to notify such third party in advance of the contents and conditions set forth in this document.
11. This document shall not be reprinted, reproduced or duplicated in any form, in whole or in part, without prior written consent of Renesas Electronics.
12. Please contact a Renesas Electronics sales office if you have any questions regarding the information contained in this document or Renesas Electronics products.
(Note 1) "Renesas Electronics" as used in this document means Renesas Electronics Corporation and also includes its directly or indirectly controlled subsidiaries.
(Note 2) "Renesas Electronics product(s)" means any product developed or manufactured by or for Renesas Electronics.

(Rev.4.0-1 November 2017)



SALES OFFICES

Renesas Electronics Corporation

<http://www.renesas.com>

Refer to "<http://www.renesas.com/>" for the latest and detailed information.

Renesas Electronics America Inc.
1001 Murphy Ranch Road, Milpitas, CA 95035, U.S.A.
Tel: +1-408-432-8888, Fax: +1-408-434-5351

Renesas Electronics Canada Limited
9251 Yonge Street, Suite 8309 Richmond Hill, Ontario Canada L4C 9T3
Tel: +1-905-237-2004

Renesas Electronics Europe Limited
Dukes Meadow, Millboard Road, Bourne End, Buckinghamshire, SL8 5FH, U.K
Tel: +44-1628-651-700, Fax: +44-1628-651-804

Renesas Electronics Europe GmbH
Arcadiastrasse 10, 40472 Düsseldorf, Germany
Tel: +49-211-6503-0, Fax: +49-211-6503-1327

Renesas Electronics (China) Co., Ltd.
Room 1709 Quantum Plaza, No.27 ZhichunLu, Haidian District, Beijing, 100191 P. R. China
Tel: +86-10-8235-1155, Fax: +86-10-8235-7679

Renesas Electronics (Shanghai) Co., Ltd.
Unit 301, Tower A, Central Towers, 555 Langao Road, Putuo District, Shanghai, 200333 P. R. China
Tel: +86-21-2226-0888, Fax: +86-21-2226-0999

Renesas Electronics Hong Kong Limited
Unit 1601-1611, 16/F., Tower 2, Grand Century Place, 193 Prince Edward Road West, Mongkok, Kowloon, Hong Kong
Tel: +852-2265-6688, Fax: +852-2886-9022

Renesas Electronics Taiwan Co., Ltd.
13F, No. 363, Fu Shing North Road, Taipei 10543, Taiwan
Tel: +886-2-8175-9600, Fax: +886-2-8175-9670

Renesas Electronics Singapore Pte. Ltd.
80 Bendemeer Road, Unit #06-02 Hyflux Innovation Centre, Singapore 339949
Tel: +65-6213-0200, Fax: +65-6213-0300

Renesas Electronics Malaysia Sdn.Bhd.
Unit 1207, Block B, Menara Amcorp, Amcorp Trade Centre, No. 18, Jln Persiaran Barat, 46050 Petaling Jaya, Selangor Darul Ehsan, Malaysia
Tel: +60-3-7955-9390, Fax: +60-3-7955-9510

Renesas Electronics India Pvt. Ltd.
No.777C, 100 Feet Road, HAL 2nd Stage, Indiranagar, Bangalore 560 038, India
Tel: +91-80-67208700, Fax: +91-80-67208777

Renesas Electronics Korea Co., Ltd.
17F, KAMCO Yangjae Tower, 262, Gangnam-daero, Gangnam-gu, Seoul, 06265 Korea
Tel: +82-2-558-3737, Fax: +82-2-558-5338